

UNCLASSIFIED

AD 416495

DEFENSE DOCUMENTATION CENTER

FOR

SCIENTIFIC AND TECHNICAL INFORMATION

CAMERON STATION, ALEXANDRIA, VIRGINIA



UNCLASSIFIED

NOTICE: When government or other drawings, specifications or other data are used for any purpose other than in connection with a definitely related government procurement operation, the U. S. Government thereby incurs no responsibility, nor any obligation whatsoever; and the fact that the Government may have formulated, furnished, or in any way supplied the said drawings, specifications, or other data is not to be regarded by implication or otherwise as in any manner licensing the holder or any other person or corporation, or conveying any rights or permission to manufacture, use or sell any patented invention that may in any way be related thereto.

41-63-4-6

CATALOGED BY DDC

AD No. 416495
8130-8382 RU-000

SD-TDR-63-138

TURBULENT DIFFUSION OF A REACTING
GAS IN THE WAKE OF A SHARP NOSED
BODY AT HYPERSONIC SPEEDS

By W. H. Webb and Leslie A. Hromas

15 APRIL 1963

416495

Contract No. AF 04(694)-1

Prepared for
HQ BALLISTIC SYSTEMS DIVISION
AIR FORCE SYSTEMS COMMAND
UNITED STATES AIR FORCE
Norton AFB, California

DDC
SEP 12 1963
TISA



SPACE TECHNOLOGY LABORATORIES, INC.
a subsidiary of Thompson Ramo Wooldridge Inc.
ONE SPACE PARK · REDONDO BEACH, CALIFORNIA

BSD-TDR-63-138

TURBULENT DIFFUSION OF A REACTING GAS
IN THE WAKE OF A SHARP-NOSED BODY AT
HYPERSONIC SPEEDS

Prepared by

W. H. Webb

and

Leslie A. Hromas

SPACE TECHNOLOGY LABORATORIES, INC.
A Subsidiary of Thompson Ramo Wooldridge Inc.
One Space Park • Redondo Beach, California

6130-6362-RU-000

Contract No. AF 04(694)-1

April 15, 1963

Prepared for

HQ BALLISTIC SYSTEMS DIVISION
AIR FORCE SYSTEMS COMMAND
UNITED STATES AIR FORCE
Air Force Unit Post Office, Los Angeles 45, California
Attention: TDC

Qualified requestors may obtain copies of this report
from DDC, Cameron Station, Alexandria, Virginia.

Prepared for
HQ BALLISTIC SYSTEMS DIVISION
AIR FORCE SYSTEMS COMMAND, USAF
Under Contract AF 04(694)-1

Prepared by: W. H. Webb
W. H. Webb
Aerosciences Laboratory
Research Staff

Prepared by: Leslie A. Hromas
Leslie A. Hromas
Aerosciences Laboratory
Research Staff

Approved by: A. G. Hammitt
A. G. Hammitt, Manager
Aerosciences Laboratory
Research Staff

SPACE TECHNOLOGY LABORATORIES, INC.
A Subsidiary of Thompson Ramo Wooldridge, Inc.
One Space Park • Redondo Beach, California

TABLE OF CONTENTS

1. Introduction
2. Analysis
 - 2.1 Solution for Wake Width
 - 2.2 Relation Between Y_f and Y_{T_f}
 - 2.3 Final Relation for Wake Width
 - 2.4 Solution of Species Diffusion Equations
 - 2.5 Equations for a Simple Dissociating Gas
 - 2.6 Ionization Kinetics
 - 2.7 Initial Conditions
 - 2.8 Simple Solutions
3. Illustrative Calculations

References

Symbols

Figures

ABSTRACT

The non-equilibrium turbulent wake of a sharp nosed body is considered. Approximate integral solutions are given for the distribution of species and for the thermal properties of the wake. The method used essentially represents an extension to the case of a reacting wake of the method of Lees and Hromas which was originally developed for an equilibrium wake.

In the chemical kinetic model studied, particular attention is paid to the processes of far downstream electron decay and the appropriate oxygen attachment reactions are investigated. Some simple explicit solutions for the species diffusion in the wake are considered and detailed numerical calculations are given for both a simple dissociating gas and for a full air chemistry calculation. Finally, the scaling laws exhibited by these calculations are discussed.

1. INTRODUCTION

Recent theoretical advances ^{1,2,3,4} in the understanding of the behavior of turbulent wakes produced by bodies traveling at hypersonic speeds have encouraged a more refined examination of such wakes. A particularly restrictive assumption which has previously been made is that the gas is chemically frozen in the wake; this assumption is certainly invalid for a large range of flight altitudes over which the wake is expected to be turbulent.⁵ Under this assumption, electron densities may be calculated for only two limiting cases: with the electrons in equilibrium at the local gas temperature or with a frozen electron concentration in the wake downstream of the wake neck, i.e., electrons which are produced in the neck are simply diluted by spreading of the wake. The large differences which occur in the resulting axial distribution of electrons for these limiting cases indicate the requirement for the inclusion of finite reaction rates in wake calculations under circumstances where non-equilibrium prevails.*

The calculational procedure suggested here represents essentially an extension of the method of Lees and Hromas ¹ to the case of a reacting gas. Briefly, the model used is that of an initially hot turbulent core rapidly expanding into a radially non-uniform inviscid enthalpy field which is invariant along streamlines. For the turbulent diffusivity, the usual "similar" form is assumed, generalized for a compressible gas by a Howarth-Dorodnitsyn density ratio factor. All laminar diffusion is ignored and all turbulent diffusivities are taken equal so that the Prandtl and Lewis-Semenov numbers are unity. The axial pressure gradient

*Examples of the divergence in results which may be obtained if the finite reaction rates in the wake are ignored are given in Figs. 15 and 16 of Ref. 1.

is dropped in the conservation equations, but taken into account in the evaluation of the local density.

With this model, the conservation of energy and species equations in boundary layer form are integrated along the wake axis and across the wake, with an assumed functional form for the radial distribution. Conservation of momentum is taken account of through relating the wake momentum defect to the body drag; no separate solution of the momentum equation is required since, under the assumptions made, the Busemann integral is available (constant total enthalpy). Integration of the energy equation then yields two equations for the unknown axis enthalpy and wake width. Integration of each species conservation equation allows the distribution of that species to be determined.

The boundary conditions required are the initial ($x = 0$) values of the species and an initial value for either the wake width or the enthalpy. Further, the enthalpy at the wake edge or "front" (denoted by subscript f) must be specified. The analysis is applied sufficiently far downstream of the wake neck for the wake velocity to be nearly uniform.* The simplicity of the model used depends mainly on the constant (in x) inviscid properties and this assumption is preserved here. To be realistic, the external flow should then be non-reacting and therefore the validity of the present analysis is restricted to sharp-nosed body wakes or to the far downstream wakes of blunt bodies.

The reacting wake has also been treated recently by Bloom and Steiger⁶, using a method similar to the above. However, results for integral solutions of the momentum rather than the energy equation were given. In these results, the wake neck compression and the effects of attachment of electrons to oxygen atoms or molecules were ignored.

*For sharp bodies at high M_{∞} , the wake may be stabilized⁵ in the neck region and a long laminar run may occur during which the velocity and stagnation enthalpy defects across the wake should diminish.

2. ANALYSIS

The boundary layer form of the required conservation equations for axisymmetric ($m = 1$) or two dimensional ($m = 0$) flow is

$$1) \quad \frac{\partial}{\partial x} (\rho u y^m) + \frac{\partial}{\partial y} (\rho v y^m) = 0$$

$$2) \quad \rho u \frac{\partial \alpha_i}{\partial x} + \rho v \frac{\partial \alpha_i}{\partial y} = \frac{1}{y^m} \frac{\partial}{\partial y} \left(\rho \epsilon y^m \frac{\partial \alpha_i}{\partial y} \right) = \dot{\omega}_i$$

$$3) \quad \rho u \frac{\partial u}{\partial x} + \rho v \frac{\partial u}{\partial y} = - \frac{dp}{dx} + \frac{1}{y^m} \frac{\partial}{\partial y} \left(\rho \epsilon y^m \frac{\partial u}{\partial y} \right)$$

$$4) \quad \rho u \frac{\partial h}{\partial x} + \rho v \frac{\partial h}{\partial y} = \frac{1}{y^m} \frac{\partial}{\partial y} \left(\rho \epsilon y^m \frac{\partial h}{\partial y} \right) + u \frac{dp}{dx} + \rho \epsilon \left(\frac{\partial u}{\partial y} \right)^2$$

The enthalpy, h , is the overall enthalpy, i.e., the sum of the thermal and formation enthalpies for each species. By convention, the formation enthalpy for molecules is taken as zero and that for atoms as negative. The notation followed here is generally identical to that of Ref. 1.

An equation of state in the form

$$5) \quad p = \frac{R}{\bar{M}} \rho T$$

is assumed, where

$$6) \quad \bar{m}^{-1} = \sum_1 \alpha_1 m_1^{-1}$$

Ignoring the dissipation and pressure gradient terms and assuming constant total enthalpy yields for 3) and 4)

$$7) \quad h + u^2/2 = H_\infty$$

$$8) \quad \rho u \frac{\partial h}{\partial x} + \rho v \frac{\partial h}{\partial y} = \frac{1}{y^m} \frac{\partial}{\partial y} \left(\rho \epsilon y^m \frac{\partial h}{\partial y} \right)$$

which, along with 1), 2), 5) constitute the equation set to be solved for the unknowns u, v, ρ, h, α_1 . Values of the inviscid pressure are assumed known from a prior solution of the inviscid flow field.

The Howarth-Dorodnitsyn transformation will be applied to the independent variable y . In the turbulent wake, the form

$$9) \quad \rho_T Y_T^m dY_T = \rho y^m dy$$

is taken; for the inviscid wake

$$10) \quad \rho_\infty Y^m dY = \rho_L y^m dy$$

2.1 Solution for Wake Width

For convenience, the solution of Reference 1 for the wake width will be rederived so that the way in which the species distribution in the gas affects this solution is exhibited. Direct integration of 1) for v gives

$$11) \quad v = -\frac{1}{\rho y^m} \frac{\partial}{\partial x} \int_0^y \rho u y^m dy$$

Multiplying 8) by y^m and integrating across the wake gives, using 11),

$$12) \quad \frac{d}{dx} \left[\int_0^{y_f} \rho u h y^m dy \right] = h_f \frac{d}{dx} \left[\int_0^{y_f} \rho u y^m dy \right] + \dot{q}_f$$

where \dot{q}_f is the heat transfer at the wake edge. This quantity is ignored in comparison with the change in h due to the spreading of the wake.

Since the analysis is to be applied where the velocity is nearly uniform across the wake, the velocity is dropped in the above expression. Then using 9), 12) may be written

$$13) \quad \frac{d}{dx} \left[\rho_f \int_0^{Y_{Tf}} (h - h_f) Y_T^m d Y_T \right] = -\rho_f \frac{Y_{Tf}^{m+1}}{m+1} \frac{dh_f}{dx}$$

It is assumed that the (known) inviscid enthalpy may be represented by

$$14) \quad \frac{h_L(Y)}{h_\infty} = 1 + H g(Y)$$

where the constant $H = \frac{h_L(0)}{h_\infty} - 1$ so that $g(0) = 1$.

For the enthalpy in the turbulent wake, the form

$$15) \quad \frac{h(Y_T, x) - h_f}{h_\infty} = B(x) G(Y_T/Y_{T_f})$$

is assumed. Here $G(0) = 1, G(1) = 0$ so that

$$B(x) = \frac{h(0, x) - h_f}{h_\infty}$$

represents the enthalpy difference across the wake, normalized by the free stream enthalpy. The enthalpy depends on x through both $B(x)$ and $Y_T(x)$. Thus, 15) amounts to a separation of variables as well as a "quasi-similarity" assumption for the Y_T dependence. The function $G(Y_T/Y_{T_f})$ is assumed known so that $B(x)$ and $Y_T(x)$ are the quantities to be solved for. Inserting 14) and 15) into 13) and integrating gives

$$16) \quad G_m \rho_f B(x) Y_{T_f}^{m+1} \Big|_0^x = \frac{-H}{m+1} \int_{g(Y_{T_f})}^{g(Y_f)} \rho_f Y_{T_f}^{m+1} dg$$

where

$$G_m = \int_0^1 G(\zeta) \zeta^m d\zeta$$

It will be useful later on to have a relation between the integral of the inviscid enthalpy and the inviscid body drag. The drag coefficient is

$$17) \quad C_D = \frac{4^{m+1}}{\rho_\infty u_\infty^2 d^{m+1}} \int_0^{\infty} \rho_L u_L (u_\infty - u_L) y^m dy$$

Since $u_L \approx u_\infty$ then the constant stagnation enthalpy in the inviscid field implies that

$$u_L (u_\infty - u_L) \approx (h_L - h_\infty)$$

Calling

$$g_{m_\infty} = \int_0^{\infty} g Y^m dY$$

then

$$18) \quad \frac{d^{m+1} C_D}{g_{m_\infty}} = \frac{4^{m+1} H}{(\gamma_\infty - 1) M_\infty^2}$$

Eqn. 16) gives one relation between $B(x)$ and $Y_{T_f}(x)$. A second relation is obtained by integrating the enthalpy equation^f along the wake axis. At the axis, 8) becomes

$$19) \quad \left(\frac{\partial h}{\partial x} \right)_{Y_{T=0}} = \frac{m+1}{\beta_T u_\infty} \approx \left(\frac{\partial^2 h}{\partial Y_T^2} \right)_{Y_{T=0}}$$

where

$$\beta_T \approx \frac{u(0,x)}{u_\infty} \approx 1$$

$$\text{and } \tilde{\epsilon} = \left[\frac{\rho(0,x)}{\rho_f} \right]^{2/m+1} \epsilon$$

Inserting 15) into 19) gives

$$20) \quad \frac{dh_f}{dx} + h_\infty \frac{dB(x)}{dx} = \frac{(m+1) h_\infty}{\beta_T u_\infty} = \tilde{\epsilon} \frac{G''(0)B(x)}{Y_{T_f}^2}$$

For the turbulent diffusivity,¹

$$\epsilon = K \left[\frac{\rho(0,x)}{\rho_f} \right]^{\frac{-1}{m+1}} [u_f - u(0)] y_f$$

where K is a universal constant. Thus,

$$\tilde{\epsilon} = \frac{K h_{\infty}}{u_{\infty}} \left[\frac{\rho(0,x)}{\rho_f} \right]^{\frac{1}{m+1}} \frac{1}{B(x) y_f}$$

and 20) becomes, using 14),

$$21) \quad H g' \frac{dY_f}{dx} + \frac{dB(x)}{dx} = \frac{(m+1) G''(0)}{\beta_T (\gamma_{\infty} - 1) M_{\infty}^2} K \left[\frac{\rho(0,x)}{\rho_f} \right]^{\frac{1}{m+1}} \frac{1}{B^2(x) y_f^2} \frac{Y_f}{Y_{Tf}^2}$$

This expression, along with 16), provide the required two equations for the unknowns $Y_T(x)$ and $B(x)$. Up to this point, the analysis is essentially a repetition of that given in Reference 1. While the boundary condition on h at the wake edge ($h = h_f$) is specified, its location is not and consequently another relation is required to render the problem determinate. This relation comes from the connection between Y_T and Y_f . In evaluating this connection, the species relations must be introduced. Of course, they will also appear in the above expressions when the density ratios are evaluated by way of the equation of state, 5).

2.2 Relation between Y_f and Y_{Tf}

Integrating the scale 9) for the turbulent wake gives

$$22) \quad \frac{y_f^{m+1}}{m+1} = \int_0^{Y_{Tf}} \frac{\rho_f}{\rho} Y_T^m dY_T$$

It will be assumed that the species mass fractions are distributed as

$$23) \quad \frac{\alpha_{i_1} - \alpha_{i_1\infty}}{\alpha_{i_1_0} - \alpha_{i_1\infty}} = \beta_1(x) Q_1(\theta_1) \quad , \quad \theta_1 = \frac{Y_T}{Y_{T_{s_1}}}$$

so that $\beta_1(0) = 1$, $Q_1(0) = 1$, $Q_1(1) = 0$

The quantities α_{i_1} are the (known) initial species mass fractions on the axis; $\alpha_{i_1\infty}$ are the free stream species. The species downstream in the wake are represented by two quantities: the axis value, $\beta_1(x)$, and a characteristic mass thickness, $Y_{s_1}(x)$. This thickness is introduced to allow the assumed profiles to adjust their relative "flatness" as the diffusion proceeds.

The formation enthalpy may be taken as

$$24) \quad \frac{h^o}{h_o^o} = \beta(x) Q(\theta), \quad \theta = \frac{Y_T}{Y_{T_s}}$$

where $\beta(x)$ is then determined from

$$25) \quad \beta(x) = \frac{\sum h_{i_1_0}^o \beta_1(x)}{h_o^o}$$

and $Y_s(x)$ from

$$26) \quad Q(\theta_f) = \frac{\sum h_{i_0}^{\circ} Q_i(\theta_{i_f})}{h_o^{\circ}}, \quad \theta_f = Y_{T_f} / Y_s$$

and h_o° is the total formation enthalpy at $x = 0$, $Y_T = 0$.

For convenience, it will be assumed that the thermal enthalpy is $C_p(T) T$; the accuracy of this approximation will be assessed later.

Inserting the above in 22) gives

$$27) \quad \frac{y_f^{m+1}}{m+1} = \frac{Y_{T_f}^{m+1}}{m+1} a_1(x) + \frac{h_{\infty}^{\circ}}{h_f} G_m B(x) a(x) Y_{T_f}^{m+1}$$

$$\text{where } a(x) = \frac{1}{G_m f(x)} \int_0^1 \frac{\mathcal{H}}{\mathcal{H}_f} \left[G(\zeta) + \frac{h_o^{\circ}}{h_{\infty}^{\circ}} \frac{\beta(x)}{B(x)} Q(\zeta \theta_f) \right] \zeta^m d\zeta$$

$$28) \quad a_1(x) = \frac{m+1}{f(x)} \int_0^1 \frac{\mathcal{H}}{\mathcal{H}_f} \zeta^m d\zeta$$

$$f(x) = 1 + \frac{h_o^{\circ}}{h_f} \beta(x) Q(\theta_f)$$

and

$$29) \mathcal{K} = \frac{R_0}{\bar{\eta} C_p}, \quad C_p = \sum_1 \alpha_1 C_{p_1}$$

The second term on the right of 27) may be related to the local wake momentum defect. Call

$$C_{D_f} = \frac{4^{m+1}}{\rho_\infty u_\infty^2 d^{m+1}} \int_0^{y_f} \rho u (u_f - u) y^m dy$$

But with $u \approx u_f$ then

$$u(u_f - u) \approx \tilde{\beta}_T (h - h_f)$$

$$\text{where } \tilde{\beta}_T = \frac{u(Y_T, x)}{u_f} \approx 1$$

and 27) becomes, at $x = 0$,

$$31) \frac{y_{f_0}^{m+1}}{m+1} = \frac{Y_{T_0}^{m+1}}{m+1} a_1(0) + \frac{(\gamma_\infty - 1) M_\infty^2}{4^{m+1} \tilde{\beta}_T} \frac{p_\infty}{p_0} C_{D_{f_0}} a(0) d^{m+1}$$

For the inviscid variable, integration of 10) gives

$$\frac{y_f^{m+1}}{m+1} = \frac{p_\infty}{p} \int_0^{Y_f} [1 + Hg(Y)] Y^m dY$$

At the origin, with $g(Y) \approx 1$,

$$32) \frac{y_{f_0}^{m+1}}{m+1} = \frac{p_\infty}{p_f} \frac{Y_{f_0}^{m+1}}{m+1}$$

Comparing 32) and 31),

$$33) Y_{f_0}^{m+1} - \frac{p_f}{p_\infty} a_1(0) Y_{T_{f_0}}^{m+1} = \delta$$

$$\text{where } \delta = \frac{(m+1) (\gamma_\infty - 1) M_\infty^2}{4^{m+1} \rho_T} \frac{h_\infty}{h_{f_0}} C_{D_{f_0}} a(0) d^{m+1}$$

Expression 33) then gives the relation between the two scales at the wake origin. However, what is needed is a relation valid for all values of x . To obtain such a relation, the postulate is made that the mass

flow in the turbulent wake differs by only an additive constant from that which would be in the inviscid wake over the same physical distance. A quantitative statement of this postulate leads to the required relation, and evaluation at $x = 0$ (eq 33) gives the additive constant.

The mass flux difference is

$$\dot{M} - \dot{M}_T = \Delta = \text{Const}$$

hence

$$34) \quad Y_f^{m+1} - \tilde{\beta}_T \frac{\rho_f}{\rho_\infty} Y_{Tf}^{m+1} = \frac{(m+1)\Delta}{2\pi^m \rho_\infty u_\infty}$$

The above then gives a relation between the two scales of the same form as 33). To be consistent, it is necessary to identify the right side of 34) with δ and also to take $\tilde{\beta}_T = a_1(0)$

The expression 33) becomes, for all x ,

$$35) \quad Y_f^{m+1} - \tilde{\beta}_T \frac{\rho_f}{\rho_\infty} Y_{Tf}^{m+1} = \delta$$

2.3 Final relation for wake width.

Returning to 16), use of 35) and 18) gives

$$36) \quad \frac{C_{D_f}}{C_{D_{f_0}}} = 1 + \frac{a(0)}{\beta_T} \frac{H}{1+H} \mathcal{D}g(Y) \frac{C_D/C_{D_{f_0}}}{(m+1)g_{m_0}} \left[(m+1)g_{m_f} \frac{\mathcal{D}g(Y)^{m+1}}{dY^{m+1}} \right]$$

where the notation \mathcal{D} means

$$\mathcal{D}g(Y) = g(Y_f) - g(Y_{f_0})$$

$$\text{also } g_{m_f} = \int_{Y_{f_0}}^{Y_f} Y^m g(Y) dY$$

Combination of these relations with 21) gives, after considerable manipulation,

$$37) \quad J(Y_f) \frac{dY_f}{dx} = - \frac{\beta_T^{\frac{2}{m+1}}}{\beta_T} \frac{K G''(0)}{G_m} \left(\frac{d}{4} \right)^{m+1} C_{D_{f_0}} \left(\frac{p}{p_\infty} \right)^{\frac{1}{m+1}}$$

$$\text{where } J = \frac{Y_f^{m-1} (Y_f^{m+1} - \delta)^{2/m+1}}{\left(\frac{p_\infty}{p} \frac{\rho_f}{\rho_\infty}\right)^{m+1} \left[\frac{\rho(0,x)}{\rho_f}\right]^{m+1}} \frac{F(Y_f)}{F_1(Y_f)} \frac{C_{Df_0}}{C_{Df}}$$

$$\text{also } F(Y_f) = 1 + \frac{1-(m+1)G_m}{(m+1)^2} \frac{g'_f}{g_{m_\infty}} \frac{C_D}{C_{Df}} \frac{(Y_f^{m+1} - \delta)^2}{Y_f^m}$$

$$38) \quad F_1 = \left(\frac{p}{p_\infty}\right)^{\frac{1}{m+1}} \frac{y_f}{Y_f} = \left[1 + \frac{(m+1)H g_{m_0} (Y_f)^{\frac{1}{m+1}}}{Y_f^{m+1}} \right]$$

$$g_{m_0}(Y_f) = \int_0^{Y_f} Y^m g(Y) dY$$

$$39) \quad \text{and } B(x) = \frac{Hg_{m_\infty}}{G_m} \frac{C_{Df}}{C_D (Y_f^{m+1} - \delta)}$$

These relations are nearly identical with those from Ref. 1. Since they are coupled by way of the density to the species diffusion equations, they cannot be solved independently.

2.4 Solution of Species Diffusion Equations

Integrating 2) across the wake gives

$$40) \quad \frac{d}{dx} \left[\rho_f \int_0^{Y_{Tf}} (\alpha_i - \alpha_{if}) Y_T^m dY_T \right] = - \frac{\rho_f Y_{Tf}^{m+1}}{m+1} \frac{d\alpha_{if}}{dx} + \frac{1}{\tilde{\beta}_T u_\infty} \int_c^{Y_{Tf}} \frac{\dot{\omega}_i \rho_f}{\rho} Y_T^m dY_T$$

if the species diffusion at the wake edge is ignored. It will be assumed that the species concentrations at the wake edge are constant; then 40) may be integrated to give

$$41) \quad \left(\frac{Y_{s_1}}{Y_{s_1_0}} \right)^{m+1} = \left[\frac{\rho_{f_0}}{\rho_f} \frac{(1 + \varphi_1)}{\beta_1(x)} \frac{Q_{im}}{Q_{im_0}} \right]$$

where

$$\varphi_1 = C_1 \int_{x_0}^x Y_{Tf}^{m+1} \left[\int_0^1 \frac{\rho_f}{\rho} \dot{\omega}_i \zeta^m d\zeta \right] dx$$

$$42) \quad C_1 = \left[\tilde{\beta}_T \rho_\infty u_\infty (\alpha_{i_0} - \alpha_{i_\infty}) Q_{im_0} \left(\frac{\rho_{f_0}}{\rho_\infty} \right)^{m+1} Y_{s_1_0} \right]^{-1}$$

$$Q_{im} = \int_0^{Y_{Tf}} \frac{Y_T^m}{Y_{T_{s_1}}^m} \left(\frac{Y_T^m}{Y_{T_{s_1}}^m} \right) Q_1 \left(\frac{Y_T}{Y_{T_{s_1}}} \right) d \left(\frac{Y_T}{Y_{T_{s_1}}} \right)$$

Another relation between $\beta_1(x)$ and $Y_{s_1}(x)$ is obtained by integrating 2) along the axis. Thus

$$43) \quad \frac{d\beta_1(x)}{dx} = \frac{m+1}{\beta_T u_\infty} \approx Q_1 \quad " (0) \quad \frac{\beta_1(x)}{Y_{s_1}^2} + \frac{\dot{\omega}_1(0,x)}{\beta_T u_\infty (\alpha_{1_0} - \alpha_{1_\infty}) \rho(0,x)}$$

Eqs. 41) and 43) represent the required relations to determine the diffusion of species; they must be solved in conjunction with expression 37) for the wake width. While the complexity of 41) and 43) suggests that the possibility of an analytical solution for the coupled problem is even more remote than for the frozen gas case, under some fairly restrictive assumptions it is possible to solve for certain species. These solutions will be given later.

Although the gas temperature does not appear explicitly in the above expressions, since the reaction rates depend on temperature, it must be known in order to obtain numerical results. In addition, the specific heats are functions of temperature. For the thermal enthalpy,

$$44) \quad h + h^0 = \sum_i \alpha_i \int_{T_r}^T C_{p_i}(T) dT$$

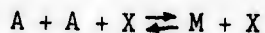
With h , h^0 , α_i known at any point in the solution, then with a known functional form for $C_{p_i}(T)$, the above gives an implicit relation to solve for the temperature.

2.5 Equations for a Simple Dissociating Gas

Since machine computation is to be applied, there is in principle no difficulty in the simultaneous solution of 37), 41) and 43) for an indefinite number of species (other than economic restrictions on computer operating time). However, in order to bring out the essential features of the problem, numerical results will mainly be given here for the case of a simple dissociating gas composed of but one molecular species. The fact that there are no available wake neck solutions which would provide initial distributions for the wake calculation also suggests the appropriateness of a simplified chemical model at this time.

The (neutral) gas model thus consists of a single atomic and molecular species. It is also possible to include charged species in a simple way. Generally, the range of temperatures which exist in the wake are sufficiently low so as to prevent a significant depopulation of the neutral species. Further, the total energy involved in producing charged species is inadequate to influence the thermodynamic behavior of the wake. Consequently, a solution for the diffusion of charged species is not required in the neutral species solution, and the ionization kinetics may be uncoupled.

The basic neutral particle reaction assumed is



where A and M denote the atomic and molecular species respectively. With but two species, only one need be solved for since conservation of mass gives the other. As shown by Fay and Riddell⁷, for the atomic

species

$$45) \quad \dot{\omega}_A = -2 k_f \frac{\rho^3}{\mathcal{M}^2} \left[\frac{(1 + \alpha)(\alpha^2 - \alpha_E^2)}{1 - \alpha_E^2} \right]$$

where α_E is the equilibrium atom mass fraction at the local temperature and pressure. From the expression for the equilibrium constant,

$$\alpha_E = \left[1 + 4 K_E \frac{\rho}{\mathcal{M}} (1 + \alpha) \right]^{-1/2}$$

and the forms

$$46) \quad K_E = a_E T^{n_E} \exp(-b_E/T), \quad k_f = a_f T^{n_f} \exp(-b_f/T)$$

are taken for the equilibrium and rate constants.

The specific heat of the atoms will be taken independent of temperature. For the molecules, the relation

$$c_{P_m}(T) = \frac{7}{2} \frac{R_0}{\mathcal{M}} \left[1 + \frac{2}{7} e^{-(T_v/T)^2} \right]$$

approximately holds. The thermal enthalpy is

$$47) \quad h + h^0 = \left[(1-\alpha) \sigma_m(T) + \frac{5\alpha R}{m} \right] T$$

$$\text{where } \sigma_m(T) = \frac{7R_0}{2mT} \int_0^T \left[1 + \frac{2}{7} e^{-(T_v/T)^2} \right] dT$$

The above may be written as

$$48) \quad \sigma_m(T) = C_{p_m}(T) - \frac{R_0}{m} \frac{T_v}{T} \Gamma_{1/2} (T_v^2/T^2)$$

where

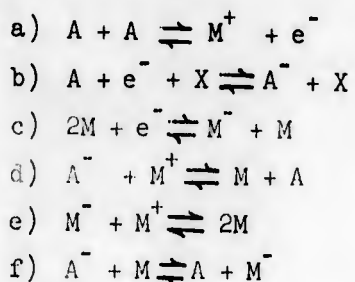
$$49) \quad \Gamma_{1/2}(T_v^2/T^2) = \int_{T_v^2/T^2}^{\infty} \frac{e^{-\lambda}}{\lambda^{1/2}} d\lambda$$

To simplify the solution of 47) for the temperature, the term 49) which is small for low temperatures will be ignored. This assumption is simply that of taking the thermal enthalpy as $C_p(T)T$ instead of $\int_0^T C_p(T)dT$. It has already been imposed implicitly in determining the initial conditions (see eq. 27).

2.6 Ionization Kinetics

The following reaction set has been chosen to represent the ionization kinetics:

50)



The first equation is the basic reaction of associative ionization and dissociative electron recombination^{8,9}. Reactions b) and c) represent two feasible electron attachment processes¹⁰. The possibility¹¹ of mutual neutralization is represented by reactions d) and e). Finally, reaction f) corresponds to the exchange of charge between the negative atomic and molecular ions.

The dominant electron removal mechanism at low air density and high electron density is the reverse of a). However, as pointed out by Lees¹⁰, under the reverse circumstances the attachment mechanism b) or c) predominates. Which one of b) or c) is more important depends on the level of dissociation. The neutralization reaction d) tends to inhibit electron removal by process a) and to increase removal by b). Similarly, neutralization reaction e) inhibits removal by a) and increases removal by c). The forward speed of d) and e) varies with the square of the charge density and the backward process requires large activation energies. As a result, these reactions are probably of little importance in the far downstream wake. Finally, reaction f) affects the relative

rates of electron removal by b) and c) in a way which depends on the direction in which it proceeds.

Since the present analysis is meant to apply to sharp bodies at or below typical re-entry velocities, the presence of positive atomic ions has been ignored. This assumption greatly simplifies the ionization model and is believed to be reasonably valid under the circumstances chosen. It is also consistent with the decoupling of charged and uncharged species kinetics.

The standard rate expressions may be written for the set of six reactions a) - f). These, when inserted as $\dot{\omega}_i$ into expressions corresponding to 41) and 43), then give the required equations to integrate to determine values of β_i for the four charged species. This integration may be done either along with the integration for the neutral species or, with the results of the latter integration as input, may be done subsequently.

It should be noted that ionization due to small amounts of contaminants added to the wake flow may easily be taken care of by simply adding the appropriate production terms to the charged air species terms and integrating as many extra equations of the form 41) and 43) as required for the contaminant species.

Radiative processes have been ignored in the kinetic model. Under the range of temperatures and pressures of interest, this appears to be a good assumption. Further, it has been assumed that the reaction rates are not affected by the fact that the flow is turbulent. This assumption involves essentially two postulates: first, that the fluctuations are sufficiently small in amplitude so that the time averaged temperature

may be used to characterize the local thermal energy of the flow; second, that the fluctuation frequencies are in such a range that the complex set of reaction processes is not disturbed by nor does it disturb the fluctuations.

2.7 Initial Conditions

In the form in which the problem has been posed, two initial conditions must be specified for the neutral species calculations. One is the initial value of the atom mass fraction, i.e., the initial dissociation level. The second is the initial value of the enthalpy or some measure of the wake width*. These conditions are interdependent and the choice of one limits the choice of the other to a certain range.

In the absence of an adequate theory for the chemical state of the gas immediately behind the wake neck, two obvious limiting cases may be assumed. The gas may be undissociated or the gas may be assumed to be in equilibrium at the local pressure and temperature; in either case, some choice must be made for the initial wake width or for the enthalpy. The initial wake width may be chosen on the basis of estimates from photographic evidence. If the wake is initially in equilibrium, it is then necessary to iterate between eqns. 38), 39), 46) and 47) to determine the initial enthalpy and atom mass fraction, for a given width.

It is possible to make rough estimates of the chemical state near the neck if the previous flow history is ignored. This may be done by comparing characteristic chemical reaction times with characteristic diffusion times. The species production terms may be put in the form

*That only one of these is required is due to the connection between the body drag and the product of **initial enthalpy defect** and wake width (see eq. 16). The initial wake drag, C_{D_0} , is estimated via the suggestions of Reference 1.

$$51) \quad \frac{dn_1}{n_1} = \frac{dt}{\tau_k(n_j, k_k)}$$

so that τ_k is the characteristic time for the k^{th} process and depends on the reaction rate, k_k , for that process as well as on other molar concentrations, n_j . The characteristic diffusion time is just

$$\tau_D = \frac{l^2}{\epsilon}$$

where the diffusivity ϵ may be either the laminar or turbulent value and l is an appropriate physical length scale. If the characteristic times are multiplied by the flow velocity, then the following approximate characteristic lengths are obtained on the wake axis near the neck

52)

Laminar diffusion:
$$L_L = \left(\frac{d^2 \rho_r}{\mu_\infty} \right) \beta_T u_\infty \left(\frac{p}{p_\infty} \right) \left(\frac{\rho_\infty}{\rho_r} \right) \left(\frac{T_\infty}{T} \right)^{1+\omega}$$

Turbulent diffusion:
$$L_T = \frac{d}{K} \frac{\beta_L \beta_T (\gamma_\infty - 1) M_\infty^2}{y_f / d} \left(\frac{1+H}{T/T_\infty} \right)^{1/2} \left[\frac{T}{T_\infty} - (1+H) \right]^{-1}$$

Ionization:
$$L_I = \left(\frac{m_\infty^{2.5}}{.64 a_I \rho_r^2 N_A} \right)^{1/2} \frac{\beta_T u_\infty n_e}{\alpha_o} \left(\frac{\rho_r}{\rho_\infty} \right) \left(\frac{p_\infty}{p} \right) \left(\frac{T}{T_\infty} \right)^{2.5} \exp\left(\frac{106}{T/T_\infty}\right)$$

Electron recombination:
$$L_{eR} = \left(\frac{N_A T_\infty^{1.5}}{a_{eR}} \right) \frac{\beta_T u_\infty}{n_e} \left(\frac{T}{T_\infty} \right)^{1.5}$$

Oxygen attachment:
$$L_A = \left(\frac{25 m_\infty^2}{\rho_r a_A} \right) \frac{\beta_T u_\infty}{(1-\alpha_o)^2} \frac{n_{O_2}}{n_e} \left(\frac{p_\infty}{p} \right)^2 \left(\frac{T}{T_\infty} \right)^2 \left(\frac{\rho_r}{\rho_\infty} \right)^2$$

Oxygen detachment:
$$L_D = \left(\frac{54M T_\infty^{1.5}}{\rho_r^a} \right) \left(\frac{\beta_T u_\infty}{1 - \beta_T} \right) \left(\frac{T_\infty}{T} \right)^{.5} \left(\frac{p_\infty}{\rho} \right) \left(\frac{\rho_r}{\rho_\infty} \right) \exp \left(\frac{17.8}{T/T_\infty} \right)$$

Oxygen dissociation:
$$L_{O_2} = \left(\frac{M T_\infty^2}{\rho_r^a} \right) \beta_T u_\infty \left(\frac{T}{T_\infty} \right)^3 \left(\frac{\rho_r}{\rho_\infty} \right) \left(\frac{p_\infty}{p} \right) \exp \left(\frac{198}{T/T_\infty} \right)$$

In the above expressions, M is the molecular weight, ρ_r is a reference density and the "a" quantities are the appropriate rate coefficients (see eqn. 46). Also

$$\beta_T = u/u_\infty, \beta_L = u_f/u_\infty, N_A = 6.02 \times 10^{23}$$

Possible numerical values for some of the parameters in the above expressions are given in the table below for the near wake neck area of a sharp and blunt body.

<u>Quantity</u>	<u>Sharp Body</u>	<u>Blunt Body</u>
β_T	.5	.2
β_L	.9	.8
p/p_∞	2	40
y_f/d	.9	.5
H	2	20

With the following choices for the other parameters, the lengths take on the values shown in Fig. 1 for different altitudes:

$T/T_{\infty} = 30$	$\omega = 1/2$
$\alpha_0 = .2$	$K = .04$
$n_e = 10^{12}$	$\gamma_{\infty} = 1.4$
$n_{O_2} = 10^3/\text{cc}$	$M_{\infty} = 22$
$d = 1 \text{ ft}$	$T_{\infty} = 300^{\circ}\text{K}$
$u_{\infty} = 22,000 \text{ ft/sec}$	$\rho_r = 1.23 \times 10^{-3} \text{ gm/cc}$
$M = 30$	$\mu_{\infty} = 4 \times 10^{-7} \text{ lb sec/ft}^2$
$a_I = 2.6 \times 10^{13}$	$\frac{\rho_r}{\rho_{\infty}}$ increases by 10 for each 50K ft altitude
$a_{eR} = 2 \times 10^{21}$	
$a_A = 10^{18}$	
$a_D = 6 \times 10^9$	
$a_{O_2} = 9.6 \times 10^{19}$	

It is apparent that; except for sharp body dissociation and ionization above 150K ft., all the characteristic chemical lengths are considerably smaller than the diffusion lengths near the wake neck when the above choices are made for the neck conditions. Thus, it may be a fair approximation to take all species to be in equilibrium near the wake neck at least below 150K ft altitude. It is then implied that a high initial electron number density will occur behind the body over a large altitude range. Thus, the principal effect of the downstream wake is the diminution of the high initial electron level by a) turbulent mixing with the (cold) inviscid stream and b) through the subsequent non-equilibrium kinetic

decay processes which operate at the low downstream temperatures induced by the mixing.

2.8 Simple Solutions

The history of electron decay in the reacting wake is a process of considerable current interest. Under some simplifying assumptions, explicit solutions may be obtained for at least part of this process. Consider the axisymmetric wake of a sharp nosed body. If but one species integral is used, so that $Y_{s_i} = Y_{T_F}$, then 43) becomes, for the electrons,

$$53) \quad \frac{d\beta_e}{dx} = \frac{2 Q'' \tilde{\epsilon}}{u_s d} \frac{\beta_e}{Y_{T_F}^2/d^2} + \frac{d}{u_s} \frac{\rho_0}{\rho} \frac{\dot{\omega}_e}{n_e m_e}$$

where $\bar{x} = \frac{x}{d}$ and the velocity constants have been taken unity. Assume that the pressure is constant, that $\rho \propto \frac{1}{T}$, and that the temperature depends on x only and is approximately uniform across the wake. For the production term, consider only the recombination and molecular attachment process so that

$$54) \quad \frac{\dot{\omega}_e}{n_e} = -k_r n_e^2 - k_a n_m^2 n_e$$

where n_m is the molecular molar density. Taking

$$k_r = \tilde{a}_r \left(\frac{T}{T_0} \right)^{-1.5} \quad (\tilde{a}_r \approx \frac{2 \times 10^{21}}{T_0^{1.5}}, \text{ see Table 1})$$

$$k_a = a_a \quad (a_a \approx 10^{18})$$

then

$$55) \quad \frac{d\beta_e}{d\bar{x}} - A(\bar{x}) \beta_e + A_1(\bar{x}) \beta_e^2 = 0$$

where

$$A(\bar{x}) = \frac{2 Q''}{Y_{T_F}^2 / d^2} \frac{\tilde{\epsilon}}{u_\infty d} - \frac{d}{u_\infty} a_a n_m^2$$

$$A_1(\bar{x}) = \frac{n_{e_0} d}{u_\infty} \tilde{a}_r \left(\frac{T}{T_0} \right)^{-2.5}$$

and 55) may be immediately solved for β_e . Observing that

$$\beta_e = \frac{n_e T}{n_{e_0} T_0}$$

then 55) becomes*

$$56) \quad \frac{1}{n_e d} = \frac{T}{T_0} f(\bar{x}) \left[\frac{1}{n_{e0} d} + \frac{\tilde{a}_r}{u_\infty} \int_{\bar{x}_0} \frac{(T_0/T)^{2.5}}{f(\bar{x})} d\bar{x} \right]$$

where $f(\bar{x}) = \exp \left(- \int_{\bar{x}_0} A(\bar{x}) d\bar{x} \right)$

Lees¹⁰ has shown that, under the same approximations, the expression 41) for the species integral across the wake also may be solved giving

$$57) \quad \frac{1}{n_e d} = \frac{Y_{Tf}^2}{Y_{Tf_0}^2} g(\bar{x}) \left[\frac{1}{n_{e0} d} + \frac{\tilde{a}_r}{u_\infty} \frac{Q_2}{Q_1} \int_{\bar{x}_0} \frac{(T_0/T)^{1.5}}{g(\bar{x})} \frac{Y_{Tf_0}^2}{Y_{Tf}^2} d\bar{x} \right]$$

where $g(\bar{x}) = \exp \left[\int_{\bar{x}_0} \frac{a_m n_e^2 d}{u_\infty} d\bar{x} \right]$

and $\frac{Q_2}{Q_1} = \frac{\int_0^1 n_e^2(\zeta) \zeta d\zeta}{\int_0^1 n_e(\zeta) \zeta d\zeta}$

*An exactly equivalent integral, with the same temperature dependence, may also be obtained for the downstream atom recombination, since $\dot{\omega}_A \sim \alpha_A^2$ (eqn 45) for small α_A . However, since the atom recombination is $\sim \rho_\infty^2$, then it will usually be negligible compared to the diffusion.

The similarity between eq. 56) and eq. 57) is apparent. In eq. 57) the term Q_2/Q_1 for the exponential profiles assumed by Lees was about 1/2. This term accounts for the effect of a non-uniform radial electron concentration on the net reaction process. The present authors have carried out a few numerical calculations to compare eq. 56) with eq. 57) for a specified temperature variation and have found only small differences between the two results.

If diffusion is ignored,

$$\frac{Y_{Tf}^2}{Y_{Tf_0}^2} = \frac{T}{T_0} = 1$$

and if Q_2/Q_1 is taken unity then both eq. 56) and eq. 57) obviously reduce to

$$58) \quad \frac{1}{n_e} = e^{\lambda(\bar{x}-\bar{x}_0)} \left[\frac{1}{n_{e_0}} + \frac{\lambda_1}{\lambda} \left(1 - e^{-\lambda(\bar{x}-\bar{x}_0)} \right) \right]$$

$$\text{where } \lambda = \frac{a n_m^2 d}{u_\infty}, \quad \lambda_1 = \frac{\tilde{a} d}{u_\infty}$$

For $\bar{x} \gg \bar{x}_0$ and also $\bar{x} \gg \lambda^{-1}$, then if $n_{e_0}^{-1} \ll \frac{\lambda_1}{\lambda}$,

$$59) \quad n_e = \frac{a}{\tilde{a} r} n_m^2 e^{-\lambda \bar{x}}$$

Thus, for a high initial concentration, the far downstream electron level decays exponentially with a coefficient proportional to the ratio between attachment and recombination rates and an exponent proportional to the attachment rate. For $u_{\infty} = 20,000$ ft/sec at 125 K ft altitude, then $\lambda^{-1} \approx 20$ so that beyond a distance of say 60 feet the exponential decay should commence. Of course, the detachment reaction will eventually enter to slow down this decay so that the exponential rate is an upper limit.¹² However, as will be shown later, should the activation energy for the reverse of the exchange reaction (50f) be negligible, the exponential decay would in fact predominate for the entire decay process. It should be noted that the above results apply for either laminar or turbulent streams, since the diffusion has been ignored. Without attachment ($\lambda=0$), eqn 58) reduces to the linear electron decay originally discussed by Lin⁸ and Feldman⁹ for the laminar wake.

For a somewhat more general limiting case, in which diffusion is considered but all the inviscid drag is contained within the wake, explicit relations for the electron decay may also be obtained. In this case, taking $Q''=G''$,

$$\frac{Y_{T_f}^2}{Y_{T_f 0}^2} = \left[1 + \Lambda (\bar{x} - \bar{x}_0) \right]^{2/3}$$

$$60) \quad \frac{2 Q'' \tilde{e} d}{Y_{T_f}^2 u_{\infty}} = \frac{2\Lambda}{3} \left[1 + \Lambda (\bar{x} - \bar{x}_0) \right]^{-1}$$

$$\frac{T(0)}{T_{\infty}} = 1 + \Lambda_1 \left[1 + \Lambda (\bar{x} - \bar{x}_0) \right]^{-2/3}$$

$$\text{where } \Lambda = - \frac{3}{16} \frac{G''}{G_1} \frac{C_D K d^3}{Y_{Tf_0}}$$

$$\Lambda_1 = \frac{(\gamma_\infty - 1) M_\infty^2}{16} \frac{C_D d^3}{Y_{Tf_0} G_1}$$

Since the quantity $f(\bar{x})$ in eq. 56) is

$$f(x) = g(\bar{x}) \exp \left[- \int_{\bar{x}_0}^{\bar{x}} \frac{2Q'' d^2}{Y_{Tf}} \frac{\tilde{\epsilon}}{u d} d\bar{x} \right]$$

$$\text{then } \frac{Y_{Tf}^2}{Y_{Tf_0}^2} g = f$$

and with the exception of the temperature ratio and Q_2/Q_1 , 56) is identical with 57). Inserting 60) into 56) gives, calling $\xi = \bar{x} - \bar{x}_0$,

$$61) \quad \frac{1}{n_e} = e^{\lambda \xi} (1 + \Lambda_1)^{-1} \left[\Lambda_1 + (1 + \Lambda \xi)^{2/3} \right] \left\{ \frac{1}{n_{e_0}} + \frac{\lambda_1}{\Lambda} (1 + \Lambda_1)^{5/2} \int_1^{1 + \Lambda \xi} \frac{\zeta e^{\lambda \zeta} (1 - \zeta)}{\left[\Lambda_1 + \zeta^{2/3} \right]^{5/2}} d\zeta \right\}$$

When $\frac{\lambda_1 - 1}{L} \ll \xi \ll \lambda^{-1}$, i.e., for large \bar{x} but with negligible attachment,

$$62) \quad \frac{1}{n_e} \approx \frac{T_\infty}{T_0} (\lambda \xi)^{2/3} \left\{ \frac{1}{n_{e_0}} + \frac{3\lambda_1}{\lambda} \left(\frac{T_0}{T_\infty} \right)^{5/2} (\lambda \xi)^{1/3} \right\}$$

The first term represents the effects of initial diffusion, the second of recombination; these contributions to the decay are equal at

$$63) \quad \xi = \frac{\left(\frac{G_1''}{G_1} \right)^2 \left(\frac{C_D K}{D} \right)^2 d^6}{3(16)^2 (\lambda_1 n_{e_0}) \left(\frac{T_0}{T_\infty} \right)^{15/2} Y_{T_0}^6}$$

It is clear that the extent of the diffusion-controlled wake depends strongly on the initial conditions chosen. When attachment predominates far downstream,

$$64) \quad n_e \approx n_{e_0} \frac{T_0}{T_\infty} (\lambda \xi)^{-2/3} e^{-\lambda \xi}$$

and, as in 59), the exponential decay is again obtained. In this case, however, the concentration and temperature at the location where attachment first predominates, as well as the diffusion parameter, determine the decay coefficient.

3. ILLUSTRATIVE CALCULATIONS

To illustrate the behavior of the reacting wake for a sharp-nosed body, calculations have been made for a range of body sizes and ambient densities for the case of a 12° cone at $M_\infty = 22$. A Kutta-Runge Adams-Moulton integration routine was used for these calculations*. This routine adjusts the integration step size so as to limit the relative error in each step to a prescribed (input) range. The range used for the calculations given here was 0.1 to 1 percent.

In most cases, the calculations given were carried out for the model gas reaction set. However, one calculation, made with a complete air chemistry set using the usual six neutral reactions with their corresponding rates¹³, is also given.

The inviscid flow field for the 12° cone was calculated from an equilibrium characteristics program (see Ref. 14). The enthalpy and pressure profiles obtained are shown in Fig. 2; these results form the input to the wake analysis.

The dissociation and enthalpy levels at the origin, i.e., near the wake neck, have been chosen arbitrarily as $\alpha_0 = 0.1$ and $B(0) = 25$, respectively. It is recognized that each of these must be a function of ambient density and body size. However, there seems to be no adequate theory at the present time from which these quantities may be obtained. The charged species were assumed to be approximately in equilibrium at the initial station. Additional calculations have been made for a range of initial concentration, α_0 , and $B(0)$ and the results of this parameter study will be given in a subsequent report.

* The computer program was written for an IBM 7090 by Maureen L. Sprankle.

With regard to the chemical reaction rates, the table below summarizes the available information on the rates of the charged particle reactions considered.*

TABLE I-REACTION RATES

<u>Reaction No.</u>	<u>Forward Rate</u>	<u>Source</u>
50 a)	$1.8 \times 10^{21} T^{1.5}$	Ref. 15
b)	$1.1 \times 10^{19} T^{-1.0}$	16
c)	1.0×10^{18}	17
d)	$1.0 \times 10^{18} T^{-.5}$	16
e)	$1.0 \times 10^{18} T^{-.5}$	16
f)	$2.1 \times 10^{12} T^{.5} \exp \left[- \frac{\Delta E_{C.E.}}{T} \right]$	16

[Units are $(\text{cm}^3/\text{gm mole})^n \text{sec}^{-1}$ where n is the reaction order and the temperature, T, is in degrees Kelvin]

In accordance with recent measurements,¹⁷ the electron affinity of molecular oxygen was taken as 0.46 electron-volts; an affinity of 1.5 eV. was taken for atomic oxygen. Thus, reaction 50f is exothermal in the reverse direction; however, whether or not an activation energy is required for the reverse reaction does not seem to be known.¹⁶ The possible range of $\Delta E_{C.E.}$ (charge exchange activation energy) is probably from about 1.5 to 1.0 eV. and each of these limits has been used in the calculations.

For the neutral gas, the high dissociation energy of nitrogen suggests that, for the range of temperatures incurred in the wake, only oxygen may be expected to dissociate to any appreciable extent. Consequently, the model gas dissociation rate chosen for the calculation herein was that

* However, Eschenroeder,¹¹ et. al., have measured an ionization rate of 1/5 of the value shown.

representative of oxygen. The numerical value for this rate was taken from Ref. 15. To attempt to simulate the air wake with the model gas reaction set, all the rates discussed above were adjusted in the calculations to account for the 20 percent-80 percent O_2-N_2 mixture of air. In addition, the NO concentration required for the reverse of reactions 50d) and c) was taken from the equilibrium calculations of Ref. 18. For all of the calculations given, only the single integral 43) was employed to determine the species concentrations; the width Y_{s_1} was taken as Y_{T_p} . A study of the effect of including two integrals will be given in a following report. The profiles of enthalpy and species distribution are inputs to the calculation and thus arbitrary; parabolas were generally chosen for each of these profiles in order to correspond to previous calculations. ^{1, 13}

Fig. 3 shows the wake growth for the range of body sizes and ambient densities calculated. The only parameter which depends on these quantities in the non-reacting wake is the initial wake drag coefficient $C_{D_f} \sim (R_{\infty,d})^{-1/2}$. This quantity has a relatively small influence on the wake. ¹ Further, the wake growth is not significantly affected by non-equilibrium phenomena since they only enter in the growth calculation through the initial conditions (which were fixed) and through the equation of state used to relate the density to pressure and temperature. As a result, the wake widths shown in Fig. 3 are very nearly identical, especially at large x/d , and the scaling parameter is $\rho_{\infty} d$.

Fig. 4 shows the mass fraction of atoms on the wake axis for different densities and body sizes. Since recombination effects are negligible in the turbulent wake of a sharp body (the characteristic length for atom recombination is orders of magnitude larger than the diffusion length),

and due to the $\rho_{\infty} d$ dependence of C_{D_f} , binary scaling is exhibited for the atom diffusion process in the turbulent wake. Thus, the curves of Fig. 4 for various $\rho_{\infty} d$ are identical at corresponding values of $\rho_{\infty} d$. Beyond the cut-off in atom production, the atom levels rapidly become independent of $\rho_{\infty} d$, i.e., diffusion prevails. It is noted that, despite the rapid diffusion of the turbulent wake (compared with laminar diffusion), a distance of over 200 body diameters is required for the atoms to be diluted by an order of magnitude in concentration. Also shown for comparison is a result for the relative atomic oxygen mass fraction from a full air chemistry calculation at $\rho_{\infty} = 10^{-6}$, $d = 1$. This calculation shows good agreement with the model gas calculation at small x/d , but diverges somewhat at lower concentration levels.

Non-equilibrium axis temperatures are shown in Fig. 5. Remarks on scaling similar to those for the atom concentrations may also be made here for the axis temperature. It is interesting that even a 1000 body diameters, the wake axis temperature is still as high as 1000°K . Fig. 6 gives the velocity ratios on the wake axis which correspond to the temperatures shown in Fig. 5. In each of these, the air calculation shows good agreement.

The wake property which is perhaps of most interest is the distribution of charged particles. In Figs. 7 and 8 are shown axis electron, as well as negative molecular and atomic ion, concentrations for three body diameters and ambient densities. The over-riding effect of non-equilibrium processes is apparent. Since electron recombination is very slow (essentially $\sim x^{-1}$), hundreds of body diameters are required for the electrons to fall to levels corresponding to critical UHF plasma frequency

($\sim 10^9$ /cc). Hence, as is well known, even though the temperature has fallen well below the temperature required to produce this level in chemical equilibrium, the electron wake persists far downstream. Eventually, attachment to molecular oxygen occurs and the electron level undergoes an abrupt cut-off. The molecular ions predominate in the attachment process since, a low temperature being required for attachment due to the small electron affinity of oxygen, no atomic species are available for attachment at the large distance at which it occurs. As shown in Figs 7 and 8, the negative atomic ions are only in evidence early in the wake history. The air calculation for the electron concentration is nearly identical to the model gas result.

An interesting feature of the electron decay process enters when the charge exchange energy, ΔE_{CE} (see Table 1), is taken as 1.0 eV, the anticipated lower limit. In this case, the charged O_2^- molecules rapidly give up their charge to the atomic oxygen. The O_2^- detachment reaction then is suppressed and the O_2 attachment reaction sharply cuts off the electron concentration, in the exponential manner suggested by eqn (1). This phenomena may be seen in Fig. 9 which shows calculations made with $\Delta E_{CE} = 1.5, 1.0$ eV and also for a case where only recombination to NO^+ was allowed. The charge exchange energy of 1.0 eV results in a sooner and much more abrupt cut-off of the electrons; the higher charge exchange energy and the simple recombination profiles extend thousands of body diameters further.

It has been pointed out by Lees¹⁰ that the simple solutions 56) or 57) indicate that the electron history should scale as

$$n_e d \sim \rho_\infty^2 d, x/d$$

In order to determine the extent to which this scaling also holds for the computations here, results for several body sizes and ambient densities are compared in Figs. 10 and 11 in terms of $n_e d$. The two cases $\rho_\infty^2 d = 10^{-10}$ and 10^{-11} are represented in these calculations. For the calculations shown in Fig. 10, $\Delta E_{CE} = 1.5$, and it is apparent that the suggested scaling does not collapse the curves. This failure of the $\rho_\infty^2 d$ scaling is due to the effect of the back or detachment reaction, which was not considered in the simple solutions. When $\Delta E_{CE} = 1.0$ is taken, so that the back reaction is suppressed, the suggested scaling is nearly perfect as shown in Fig. 10 for two of the cases of Fig. 9. Finally, it is noted that small differences still occur in the early electron history; these result from effects of initial dissociation and C_{Df_0} both of which scale with $\rho_\infty d$, rather than $\rho_\infty^2 d$.

ACKNOWLEDGEMENT

The authors gratefully acknowledge their stimulating discussions with Professor Lester Lees, of the California Institute of Technology and Dr. A. G. Hammitt of Space Technology Laboratories, Inc.

REFERENCES

1. Lees, Lester and Hromas, L.A., "Turbulent Diffusion in the Wake of a Blunt-Nosed Body at Hypersonic Speeds", STL Report 6110-0004-MU000 July, 1961. Also J.A.S., 29, 8 p. 976 (1962)
2. Steiger, M.H. and Bloom, M.H., "Three-Dimensional Effects in Viscous Wakes", IAS Paper 62-102, Presented at IAS National Summer Meeting June 19-22, 1962. Also J. Fl. Mech., 14, 2 P. 233, 1962.
3. Lykoudis, P.S., "The Growth of the Hypersonic Turbulent Wake Behind Blunt and Slender Bodies", RAND Memo RM-3270-PR, Jan. 1963
4. Short, W.W., "An Approximate Theory for Turbulent Wakes Behind Hypersonic Blunt Bodies", Convair Rept. 3 Ph-107, April, 1961
5. Webb, W.H., Hromas, L.A., and Lees, L., "Hypersonic Wake Transition", AIAA Journal 1,3, p. 720 (1963)
6. Bloom, M.H. and Steiger, M.H., "Diffusion and Chemical Relaxation in Free Mixing", IAS Paper No. 63-67, Presented at the IAS 31st Annual Meeting, New York, Jan. 21-23, 1963
7. Fay, J.A. and Riddell, F.R., "Theory of Stagnation Point Heat Transfer in Dissociated Air", J.A.S. 25, p. 73 (1958)
8. Lin, S.C. "Ionized Wakes of Hypersonic Objects", AVCO Everett Research Report 151, June, 1959. Also, Lin, S.C. and Teare, J.D., AVCO Everett Research Note 223, August, 1961.
9. Feldman, S. "Trails of Axi-Symmetric Hypersonic Blunt Bodies Flying through the Atmosphere", AVCO Everett Research Report 82, December, 1959
10. Lees, Lester, "Hypersonic Wakes and Trails", ARS Paper 2662-62 Presented at ARS 17th Annual Meeting, Los Angeles, November 13-18, 1962
11. Eschenroeder, A., et al, "Shock Tunnel Studies of High Enthalpy Ionized Air Flows", Chapter 11, p. 215 of High Temperature Aspects of Hypersonic Flow, Pergamon, London (1963)
12. Feldman, S. "Some Numerical Estimates of Turbulent Electron Trails", RN 8, Heliodyne Corp. Jan. 1963

13. Hall, J.G., Eschenroeder, A.Q., and Marrone, P.V., "Blunt-Nose Inviscid Airflows with Coupled Non-Equilibrium Processes", J.A.S., 29, 9, p. 1038 (1962)
14. Hromas, L.A. and Lees, L., "Effect of Nose Bluntness on the Turbulent Hypersonic Wake", STL Report 6130-6259-KU-000, October, 1962.
15. Lin, S.C. and Teare, J.D. "Rate of Ionization Behind Shock Waves in Air", AVCO/Everett Research Report 115, 1962
16. Nawrocki, P.J., "Reaction Rates", Aerophysics Corp. of America Report 61-2-A, ASTIA Catalog AD252534, 1961
17. Chanin, L.M., Phelps, A.V., and Biondi, A.V., "Measurements of the Attachment of Low-Energy Electrons to Oxygen Molecules", Phys Rev, 128, 1, p. 219 (1962)
18. Gilmore, F.R., "Equilibrium Composition and Thermodynamic Properties of Air to 24,000 K, RAND Report RM-1543, August, 1955.

LIST OF SYMBOLS

$B(x)$	$\frac{h(0,x)-h_f}{h_\infty}$
C_D	Inviscid wake drag coefficient (eq 17)
C_{D_f}	Turbulent wake drag coefficient (eq 30)
C_p	Specific heat
d	Body diameter
g	Inviscid enthalpy radial distribution function (eq 14)
G	Turbulent enthalpy radial distribution function (eq 15)
h	Thermal and chemical enthalpy
h^o	Formation enthalpy
H	$\frac{h_L(0)}{h_\infty} - 1$
k	Reaction rate
K	Universal diffusion constant
L	Characteristic length
m	Two dimensional or axi-symmetric exponent
\dot{m}	Mass flux
M	Mach number
\mathcal{M}	Molecular weight
$\overline{\mathcal{M}}$	Mean molecular weight (eq 6)
n_e	Axis electron density
p	Pressure
\dot{q}_f	Heat transfer at edge of wake
Q	Species radial distribution function (eq 23)
$R_{\infty,d}$	Reynolds number based on free stream conditions and body diameter
R_o	Gas constant

LIST OF SYMBOLS (continued)

T Temperature
 u Axial velocity
 v Radial velocity
 x Axial coordinate
 y Radial coordinate
 Y Howarth-Dorodnitsyn scale (eq 9,10)

α Species mass fraction

β_T $u(0,x)/u_\infty$

$\widetilde{\beta}_T$ $u(Y_T, x)/u_f$

β_i $\frac{\alpha_i(0,x) - \alpha_{i_\infty}}{\alpha_{i_0} - \alpha_{i_\infty}}$ (eq 23)

γ Specific heat ratio

ϵ Turbulent diffusivity

ρ Density

τ Characteristic time

$\dot{\omega}_i$ Species production term, $d(\alpha_i \rho)/dt$

Subscripts

A refers to atomic species

E Equilibrium value

f Denotes edge of wake; also forward reaction rate

i Denotes i^{th} species

k k^{th} reaction

L Inviscid flow quantity

O Quantity at wake origin ($x=x_0$)

LIST OF SYMBOLS (Continued)

- r Reference quantity
- T Turbulent flow quantity
- V Denotes characteristic vibrational temperature

LIST OF FIGURES

1. Characteristic Lengths for the Reacting Wake of A Hypersonic Body
2. Inviscid Enthalpy Profile, $g(Y)$, and Pressure History, p/p_{∞} , for 12° Cone at $M_{\infty} = 22$
3. Wake Width for 12° Cone at $M_{\infty} = 22$
4. Relative Axis Atom Mass Fraction for 12° Cone at $M_{\infty} = 22$
5. Axis Temperature History for 12° Cone at $M_{\infty} = 22$
6. Axis Velocity Ratio for 12° Cone at $M_{\infty} = 22$
7. Axis Charged Particle Concentrations for Several Ambient Densities, 12° Cone at $M_{\infty} = 22$
8. Axis Charged Particle Concentrations for Several Body Sizes, 12° Cone at $M_{\infty} = 22$
9. Effect of Charge Exchange Energy on Axis Particle Concentrations, 12° Cone, $M_{\infty} = 22$
10. Scaling With $\rho_{\infty}^2 d$ for $\Delta E_{CE} = 1.5$
11. Scaling With $\rho_{\infty}^2 d$ for $\Delta E_{CE} = 1.0$

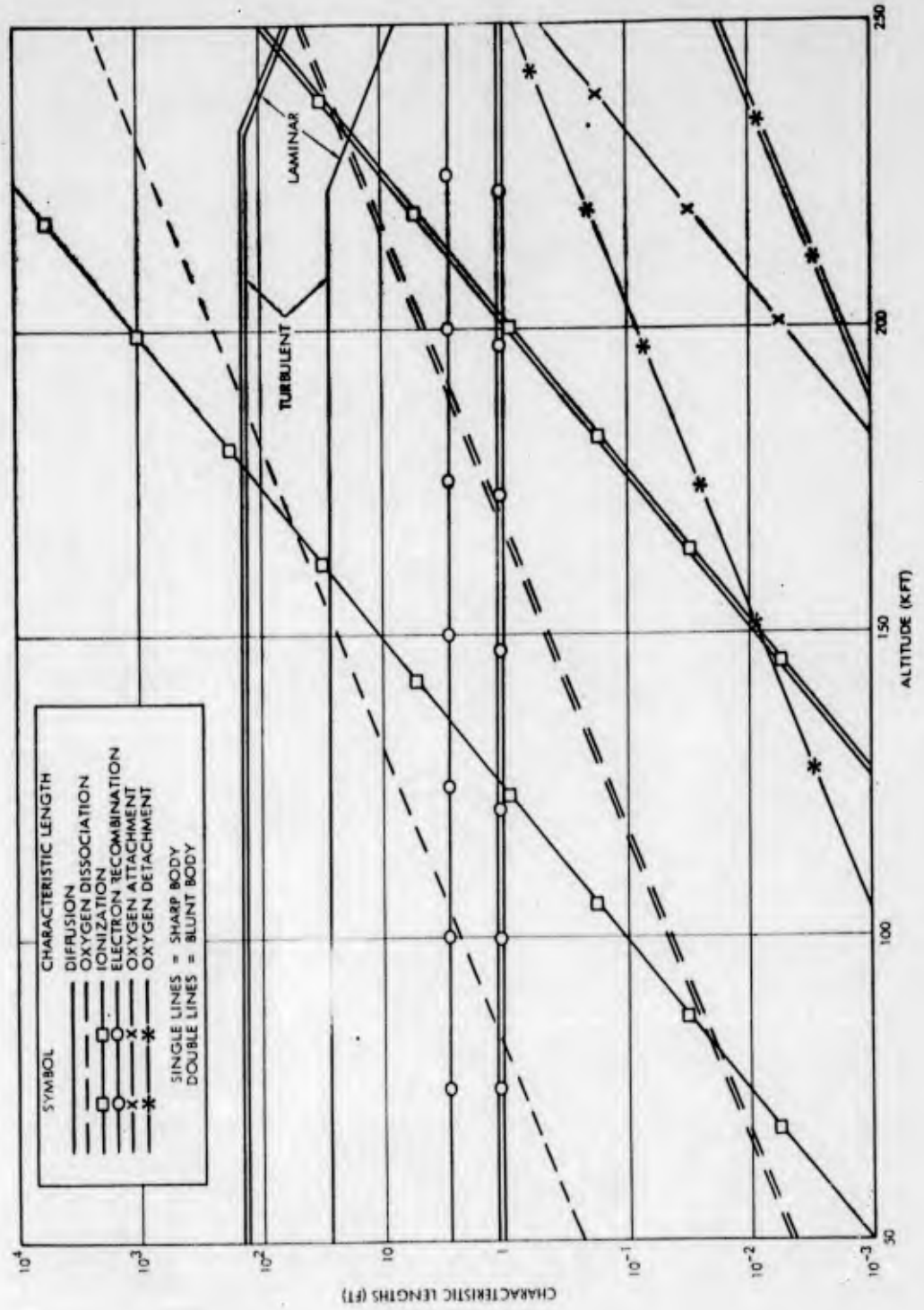


Figure 1
Characteristic Lengths for the Reacting Wake of a Hypersonic Body

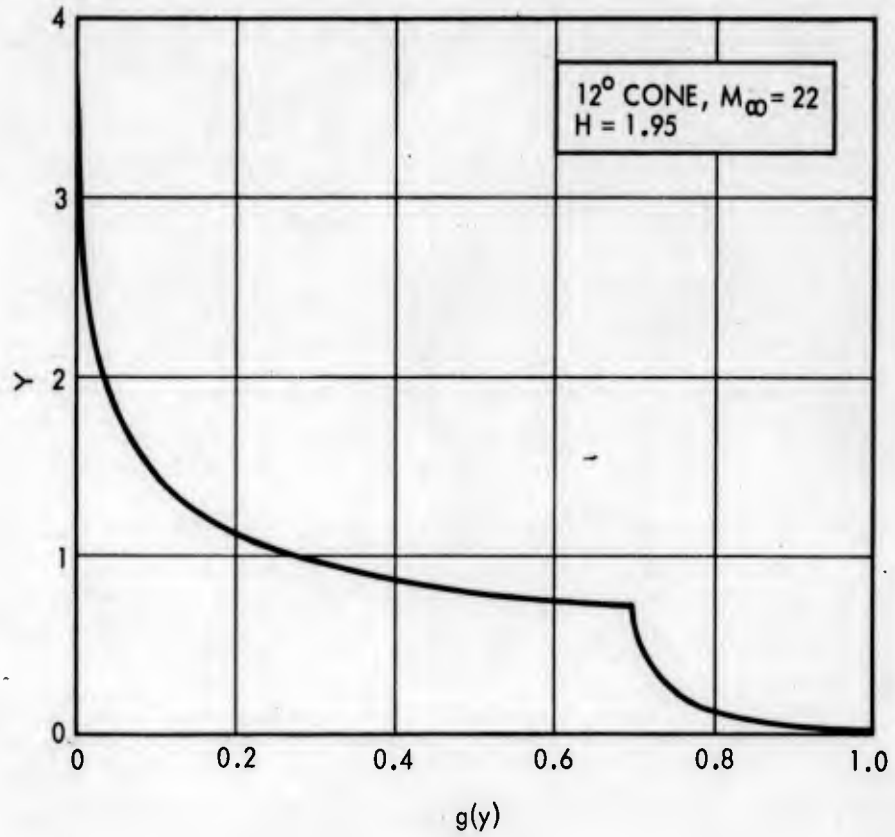
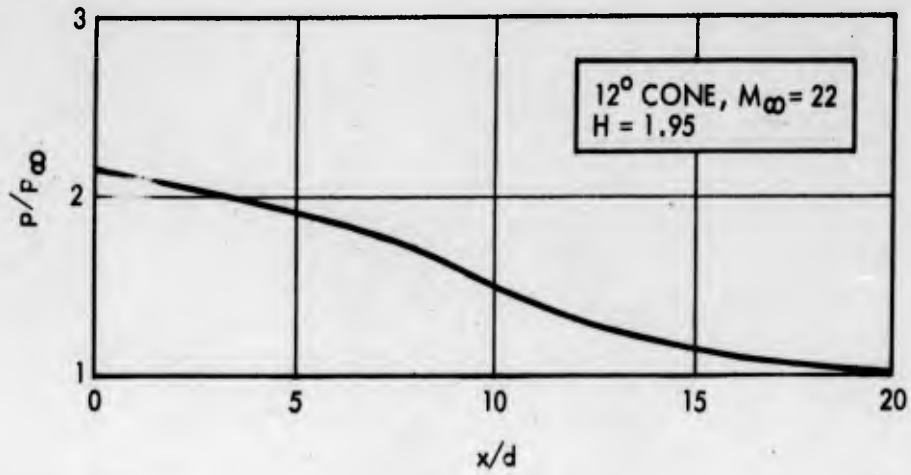


Figure 2
 Inviscid Enthalpy Profile, $g(Y)$, and Pressure History, p/p_∞ , for 12°
 Cone at $M_\infty = 22$

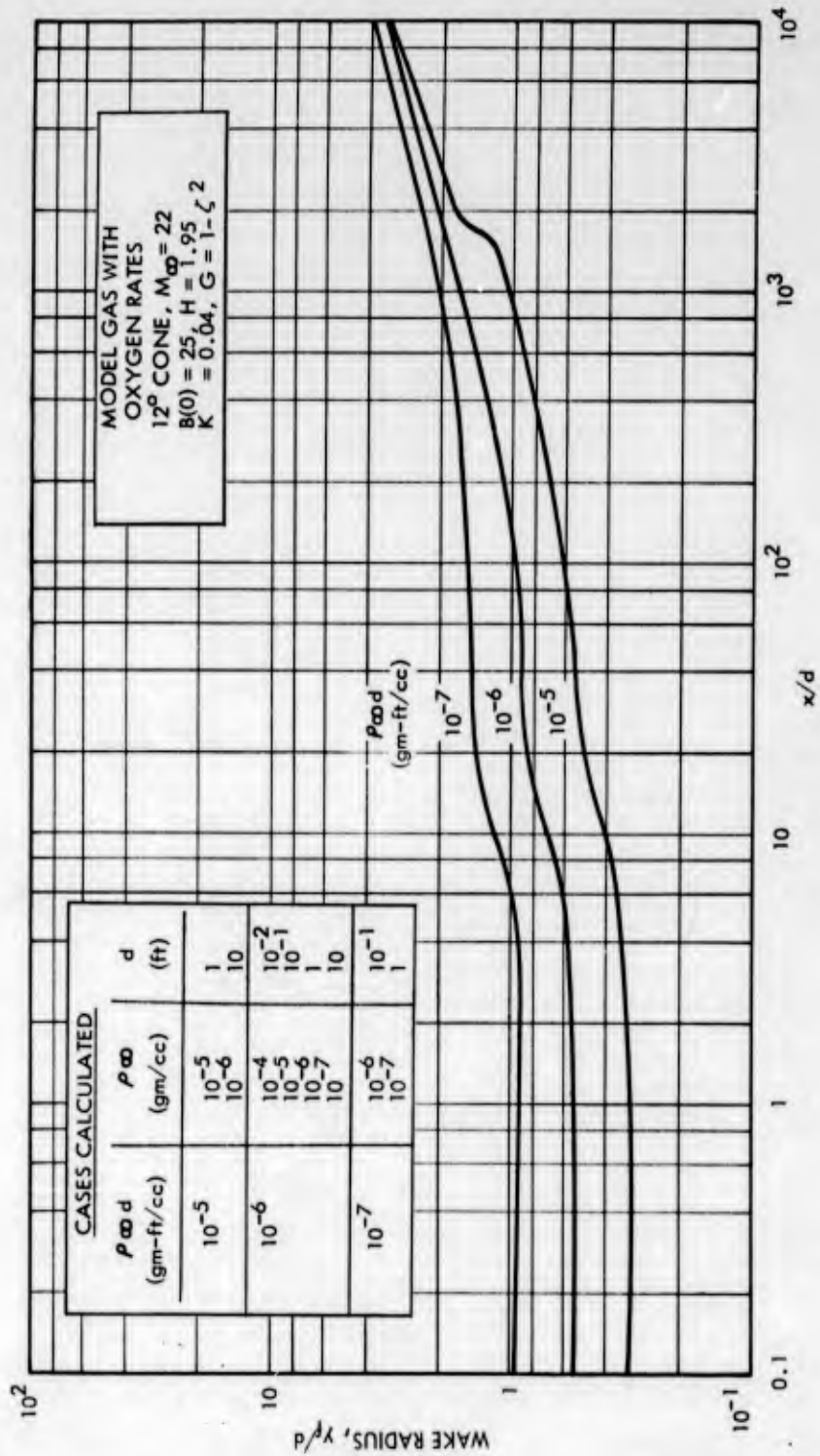


Figure 3
 Wake Width for 12° Cone at $M_\infty = 22$

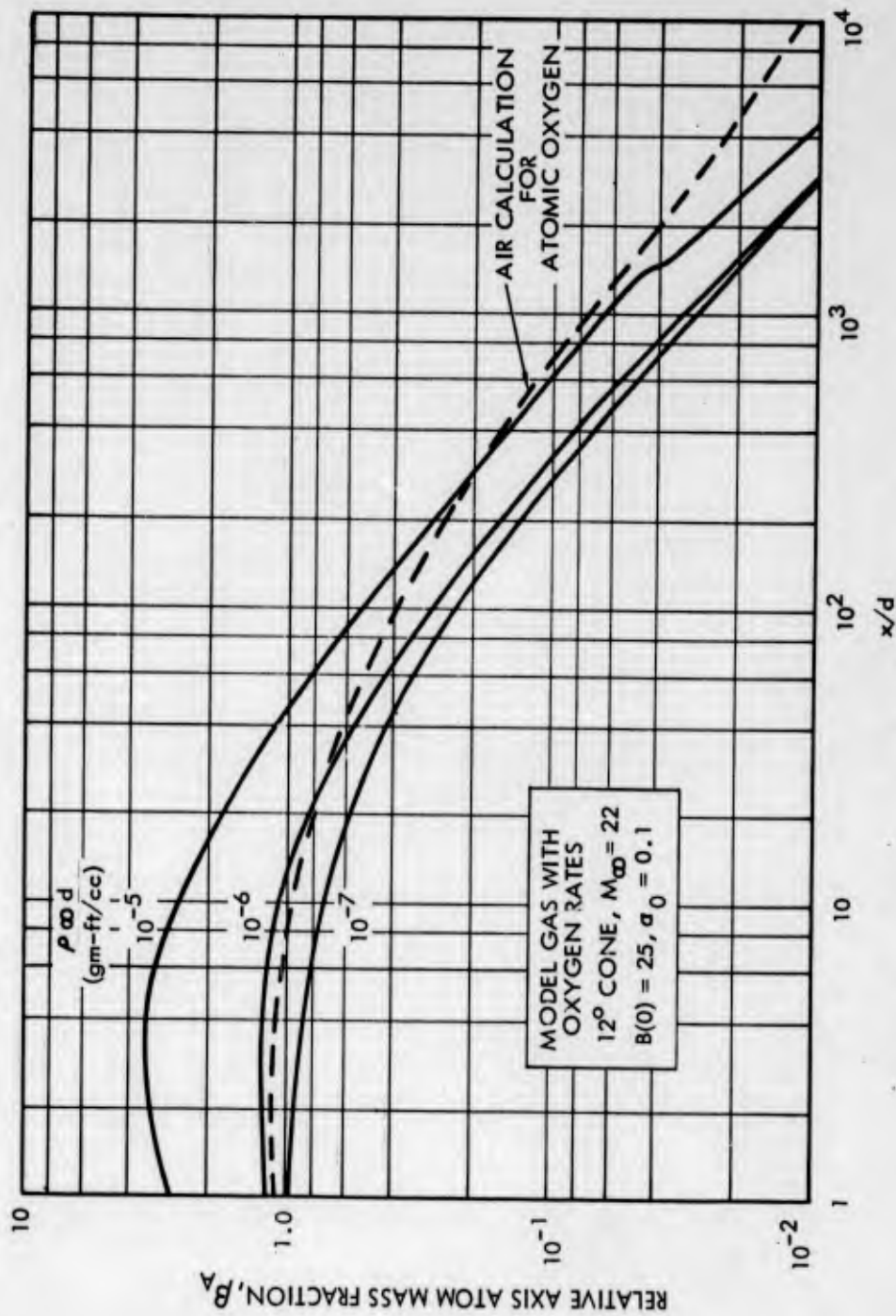


Figure 4
 Relative Axis Atom Mass Fraction for 12° Cone at $M_\infty = 22$

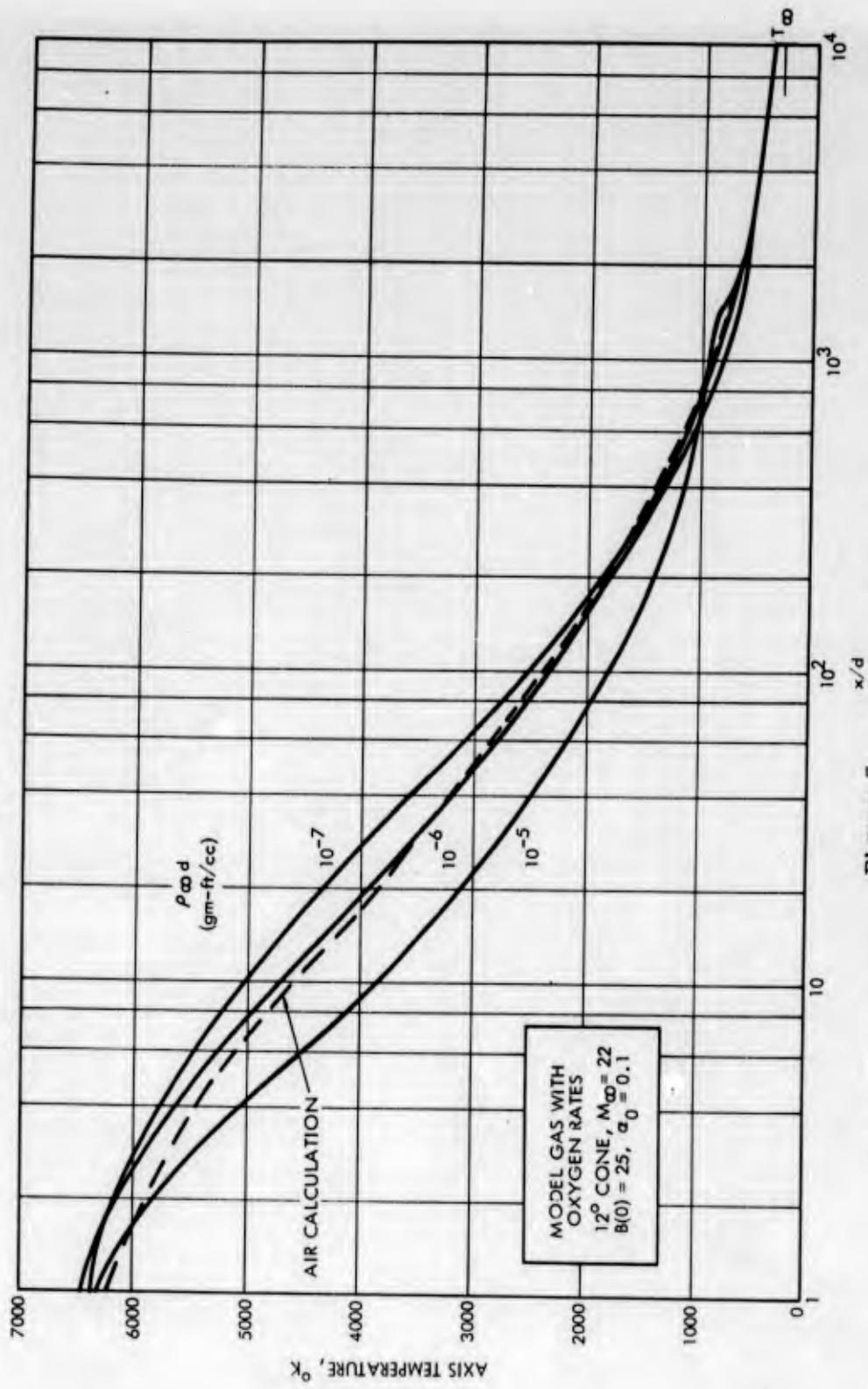


Figure 5
Axis Temperature History for 12° Cone at $M_{\infty} = 22$

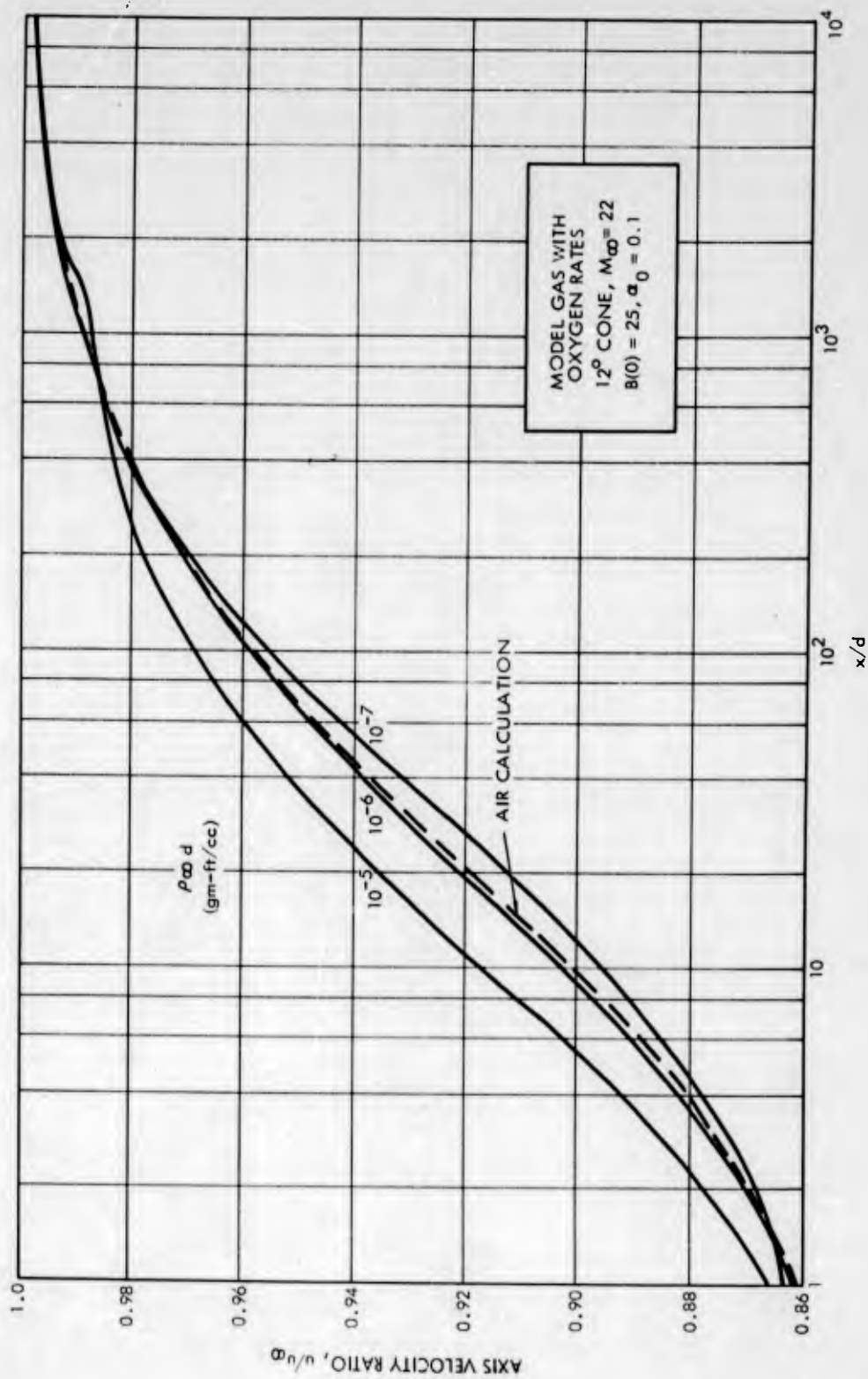


Figure 6
Axis Velocity Ratio for 12° Cone at $M_\infty = 22$

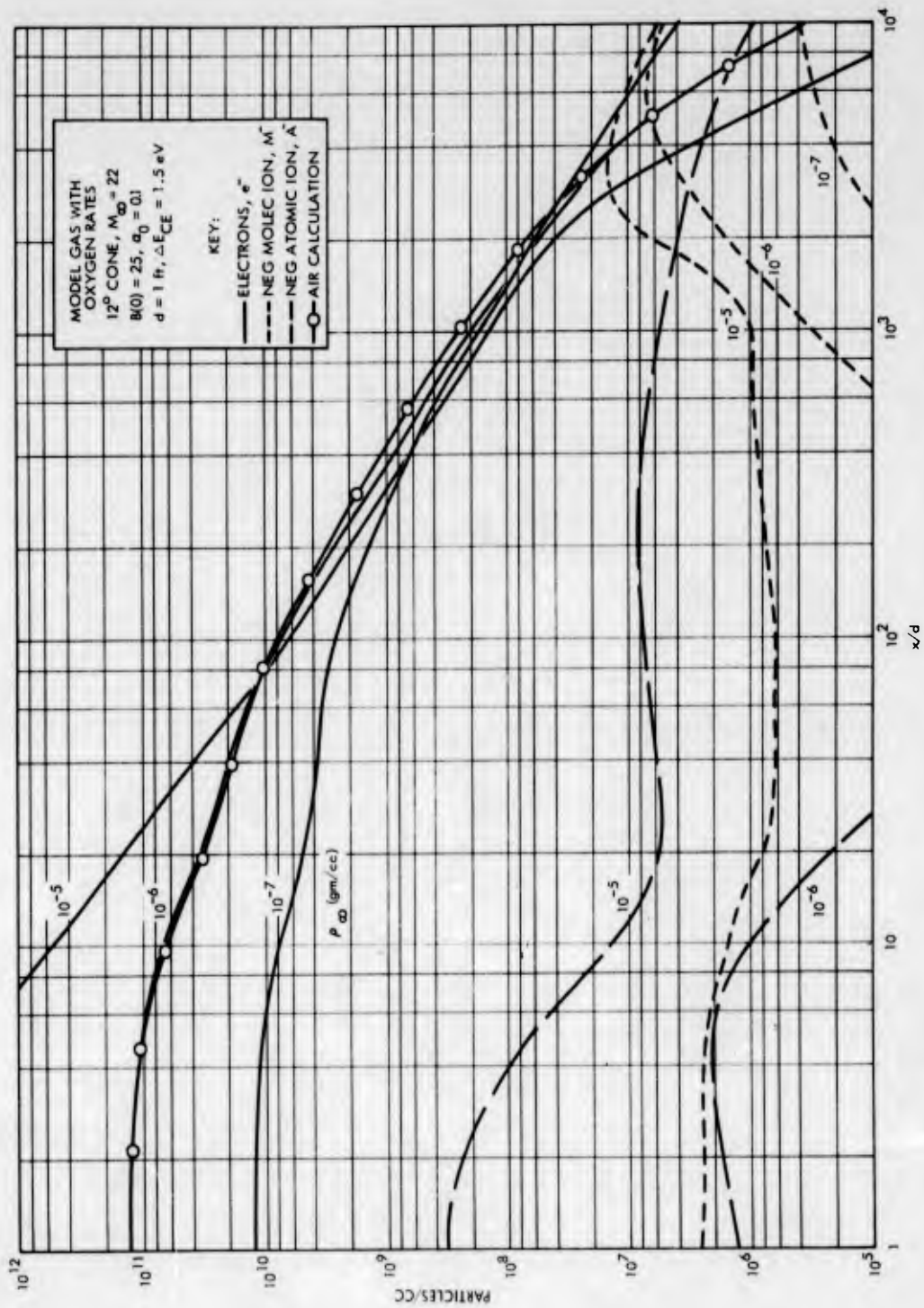


Figure 7
 Axis Charged Particle Concentrations for Several Ambient Densities,
 12° Cone at $M_\infty = 22$

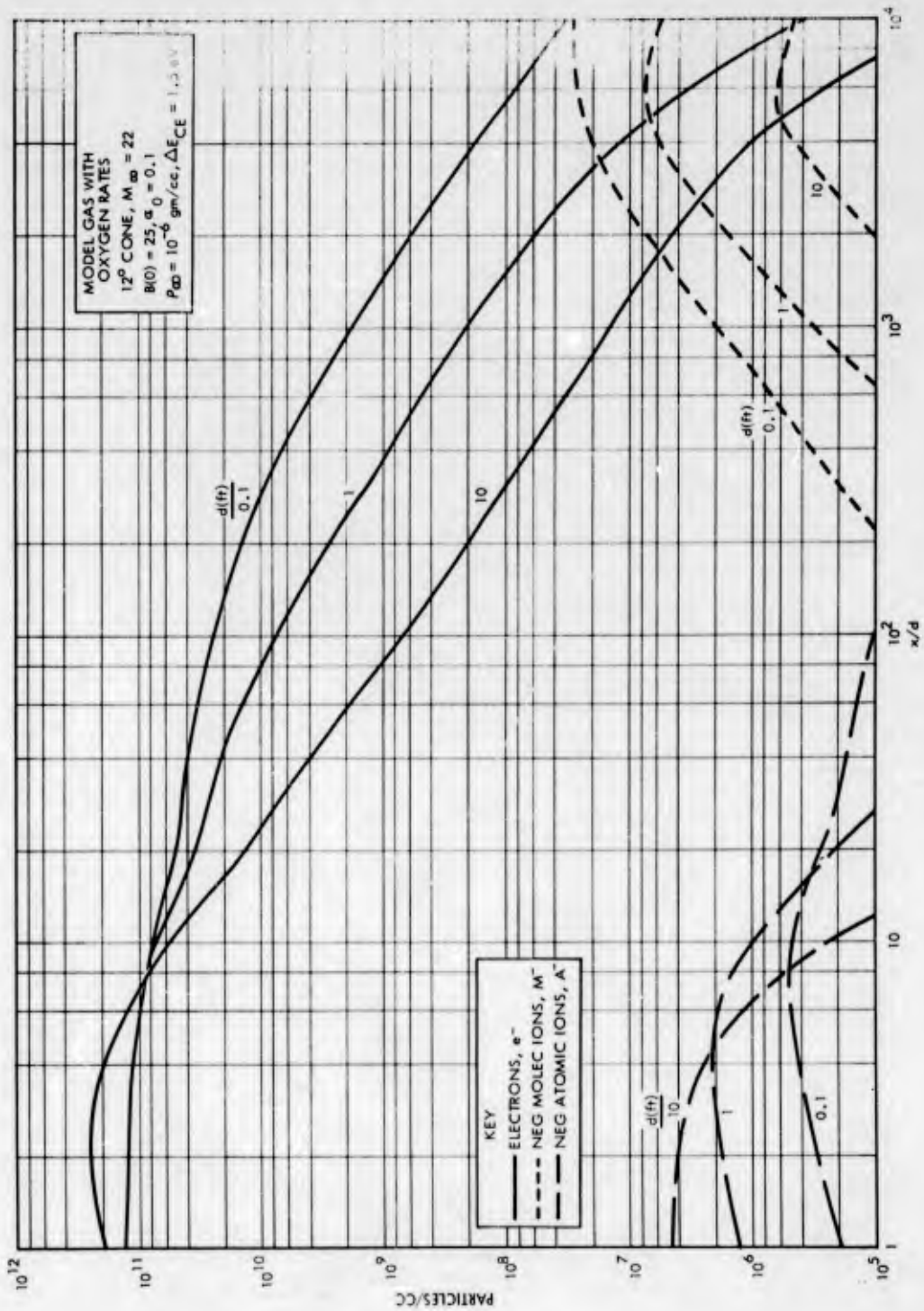


Figure 8
 Axis Charged Particle Concentrations for Several Body Sizes, 12° Cone at $M_\infty = 22$

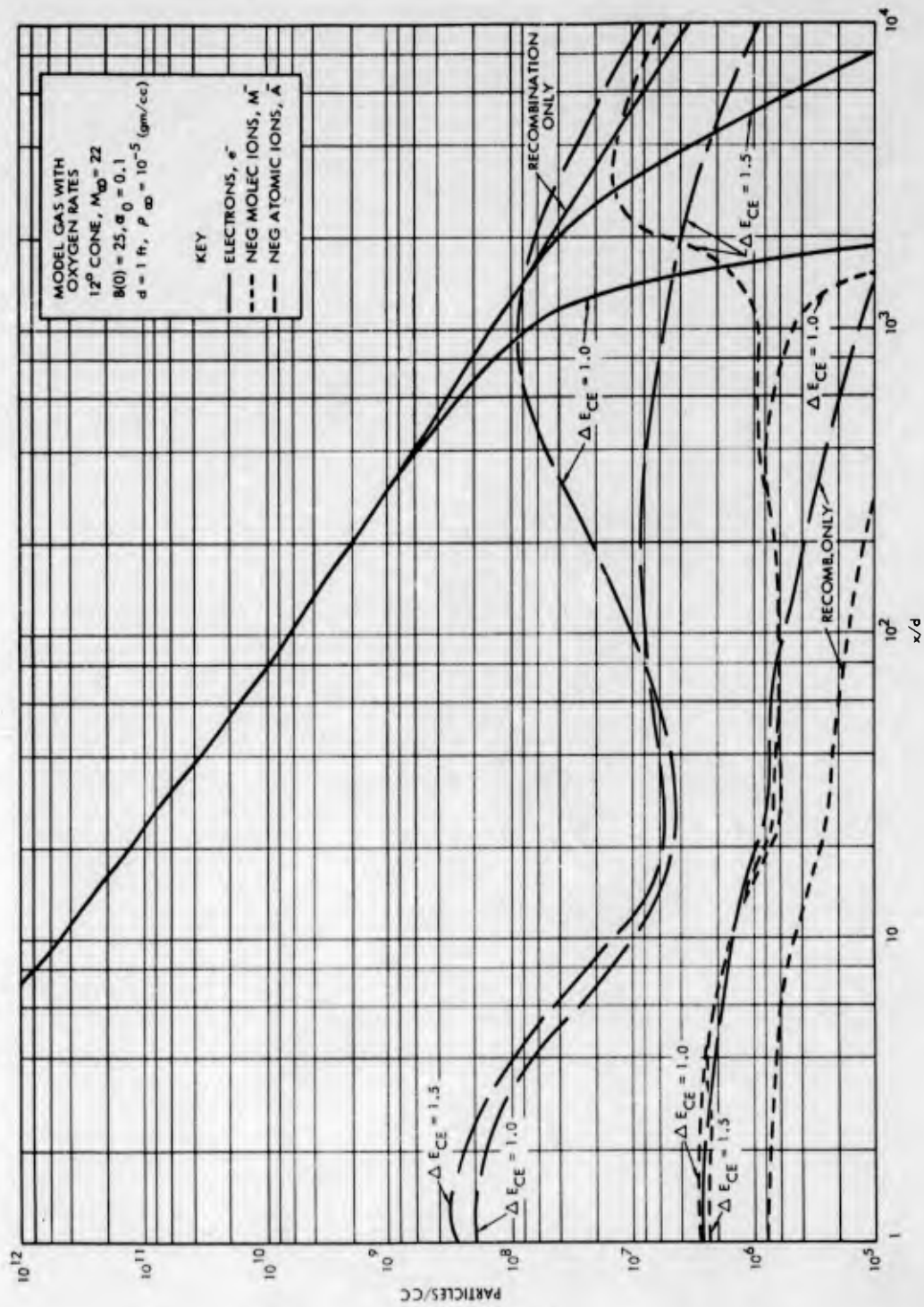


Figure 9
 Effect of Charge Exchange Energy on Axis Particle Concentrations, 12° Cone, $M_{\infty} = 22$

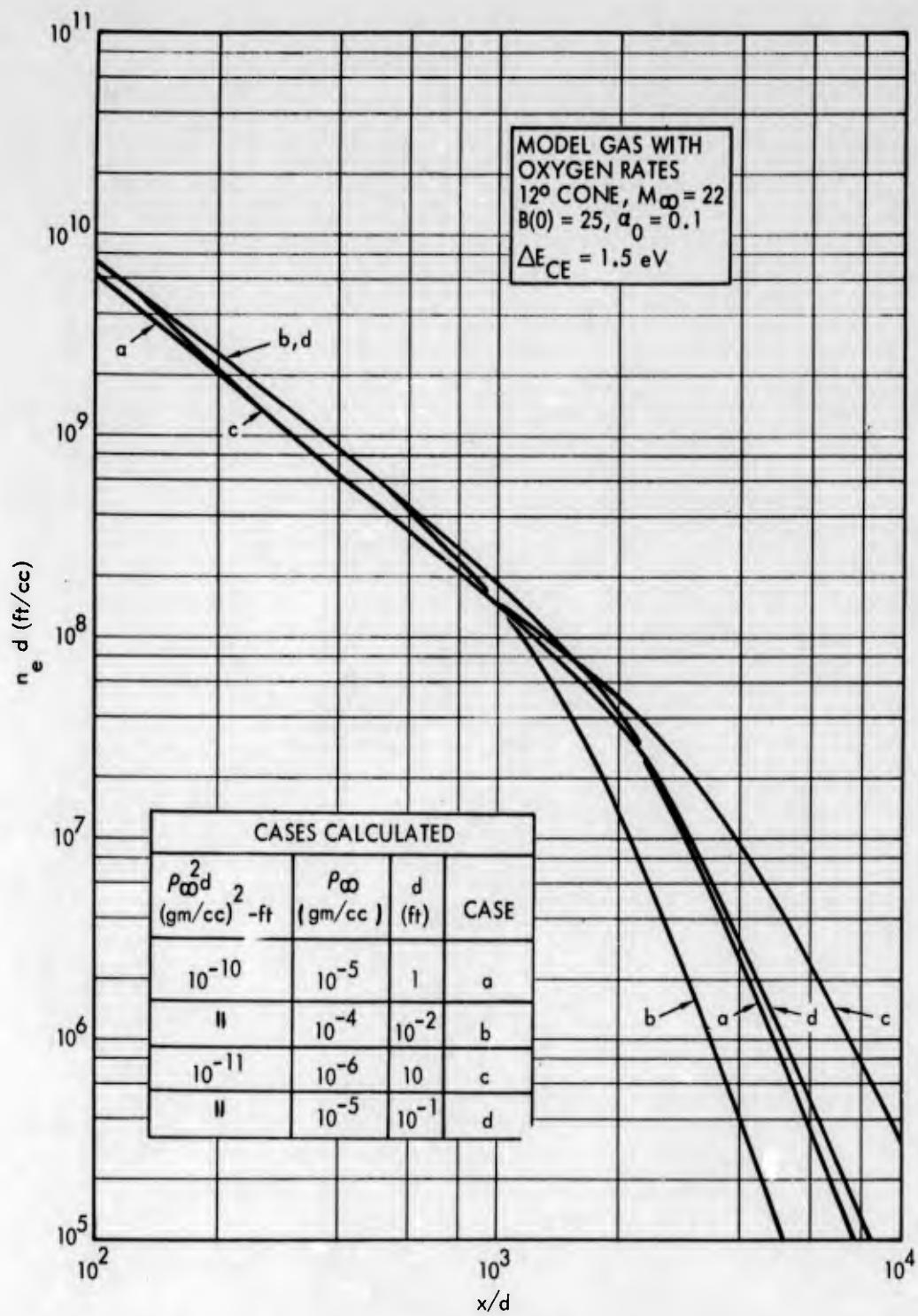


Figure 10
Scaling with $\rho_\infty^2 d$ for $\Delta E_{CE} = 1.5$

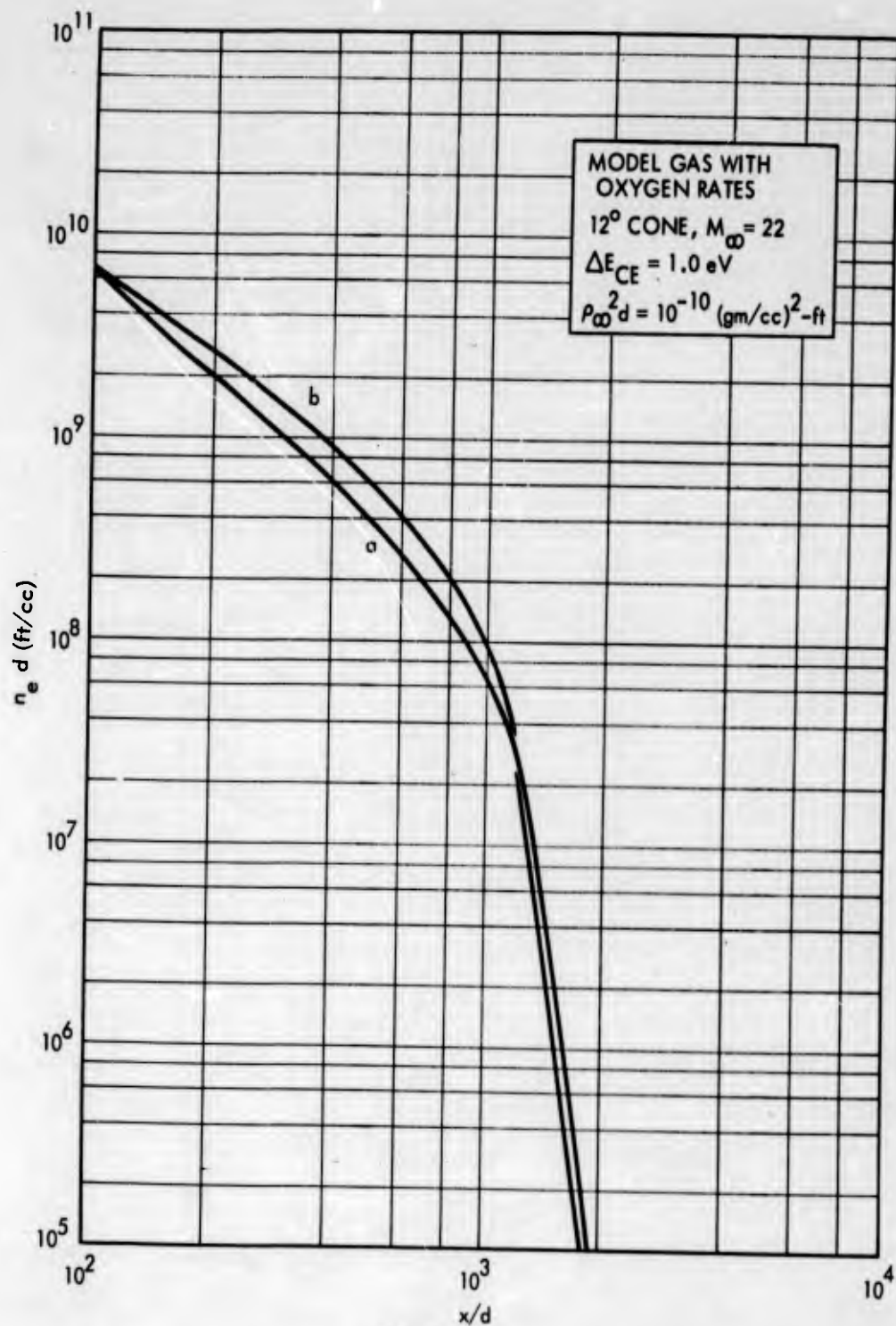


Figure 11
 Scaling with $\rho_\infty^2 d$ for $\Delta E_{CE} = 1.0$

~~UNCLASSIFIED~~

~~UNCLASSIFIED~~